5. Victoria's changing climate

This chapter lays out the observed past changes and projected future changes in many climate variables, including temperature, rainfall, temperature and rainfall extremes, wind and sea level. The chapter reports on the new high-resolution VCP19 climate projections but presents this alongside previous data sources including VicCI. New insights from the high-resolution regional climate modelling, including an enhanced drying over mountain slopes and hotter maximum warming projections are highlighted.

When interpreting climate simulations, it should be noted that projected change can be understood in the three dimensions of climate projections: internal variability, emissions scenario and climate model response. There will be ongoing climate variability through this century, at scales from seconds to decades and beyond. The other two dimensions become progressively more important through time. In this chapter the projected changes in the climate averages and the average incidence of certain climate extremes are described, focused on two main emissions scenarios and four future time periods. The nature of the climate shifts is illustrated by giving the change under a high emission scenario for a far future timeframe.

Changes to the climate have far-reaching and important impacts and present some opportunities. This chapter covers the changes in the averages and extremes of some common climate variables including temperature, rainfall, wind and fire weather. The projections do not explore the impact these changes have, including the social, economic and environmental dimensions.

5.1 Climate features and drivers

Human effects such as an enhanced greenhouse effect leading to climate change is projected to drive changes to the energy balance and related physical processes of the climate system. These changes have flow-on effects to the atmospheric circulation of the southern hemisphere, including over Victoria. Persistent shifts in the amplitude or timing of the major modes of climate variability may also occur (see Chapter 3). These changes would affect the climate of Victoria in terms of averages, variability and extremes.

Some changes are clearer than others, and the most confident projections are those linked directly to the change in greenhouse gases in the atmosphere, and the warming effect this has. However, a major projection with important implications for Victoria is a weakening and/or southerly movement of the westerly circulation and associated weather systems. Examples of this include the subtropical jet, the instability in the atmosphere that leads to the growth of weather systems, and the strength and location of the track where weather systems occur in the subtropical jet region. A reduction of blocking events and the movement of the peak of blocking further east away from Australia in winter are also projected. There is a range of projected change in these features, and there is some evidence that the projected change in these features leading to little change in rainfall is less plausible than that leading to a significant rainfall reduction (Grose et al. 2017a; Grose et al. 2019a), and with further evidence we may be able to confidently give a narrower range of plausible change and rule out the wetter end but at the moment the entire range should be considered plausible.

Changes in such features at the broad scale can interact with Victoria's physical environment – such as coastlines and mountain ranges – causing regional change. For example, a warmer atmosphere and changes to the atmospheric flow over the Australian Alps is expected to drive an enhanced rainfall reduction on the inland slopes of the Alps (see section 5.3; and Grose et al. 2019b). Further analysis of drivers important to climate change in Victoria are covered in Chapter 3, and in VicCI outputs.

5.2 Temperatures

5.2.1 Observed

Mean annual temperature has risen in Victoria in recent decades (Figure 16). The Bureau of Meteorology's official temperature trend data set, ACORN-SATv2 (Trewin 2013), shows the rate of increase is 0.1°C/decade between 1910 and 2018, resulting in an increase of just over 1°C in that period (the exact value is 1.2°C but there is some observed uncertainty around this exact number). There have been many more warm years than cool years in recent decades, and the last year with below-average temperature (using the 1961–1990 baseline) was 1996 (Figure 16). This change is similar to the Australian and global averages of a little over 1°C (Bureau of Meteorology and CSIRO 2019).

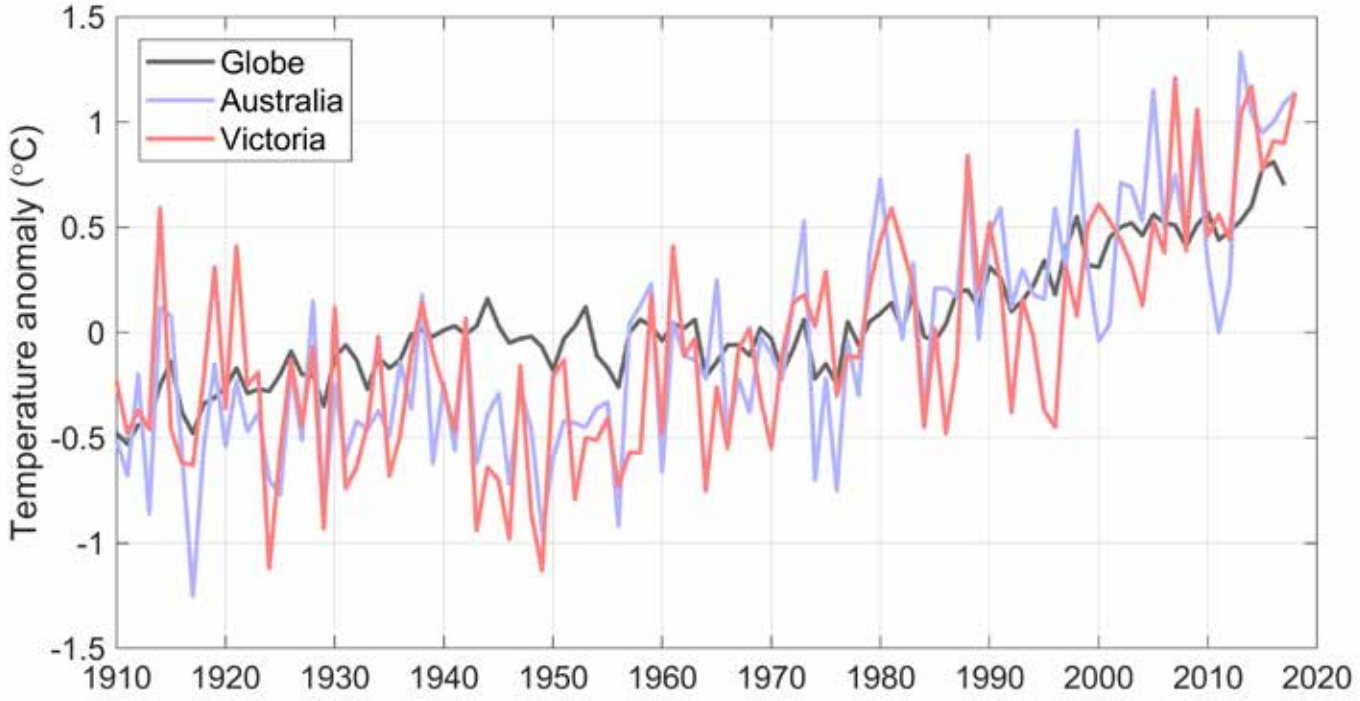

Figure 16. Annual temperature anomaly from the 1961–1990 average for the globe (HadCRUT4 data set), Australia and Victoria (ACORN-SATv2 data set)

The rate of temperature change across Victoria has accelerated in recent decades to 0.2°C/decade in the period 1950–2018 (Figure 17), at least partly due an acceleration of the enhanced greenhouse effect due to human emissions, but also with a contribution from natural variability. The baseline period used in this report is 1986–2005 (i.e. 20 years, centred on 1995). The warming prior to this was 0.06°C/decade between 1910 and 1995 (a total increase of 0.5°C). In the most recent 20 years from 1999 to 2018, the rate of warming was 0.32°C/decade (solid red line in Figure 17), however the period is too short to be considered a reliable quantification of climate change trend, since variability plays a large role.

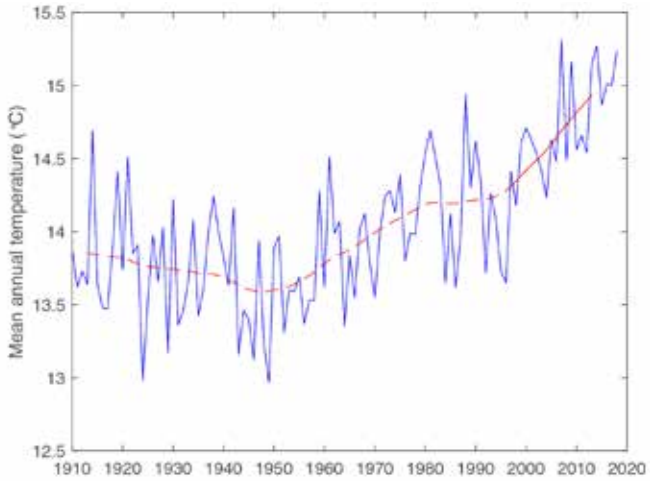

Figure 17. Mean annual temperature of Victoria with an 11-year running average shown in dashed red (the linear trend in the 20 years of 1999–2018 shown as a solid line).

The global gridded temperature data sets closely match the changes seen in ACORN-SATv2 in the period since 1910, for example, GISTEM ERSSTv5 (GISTEMP_Team 2019) and Berkeley (Rohde et al. 2013) indicate 0.1°C/decade since 1910. These data sets extend before 1910 using interpolation and statistical gap-filling to produce spatial and temporal coverage of this period using very sparse inputs. Therefore, because data prior to 1910 are considerably more limited, changes are more uncertain. The global gridded temperature data sets differ in the patterns of variability and change in the period 1850–1910 (Figure 18). Nonetheless, they broadly agree on some aspects of variability, such as relatively cooler periods in 1850–1870 and 1900–1910, and a relatively warm period in 1880–1900 but still with relatively few years above the 1961–1990 baseline mean.

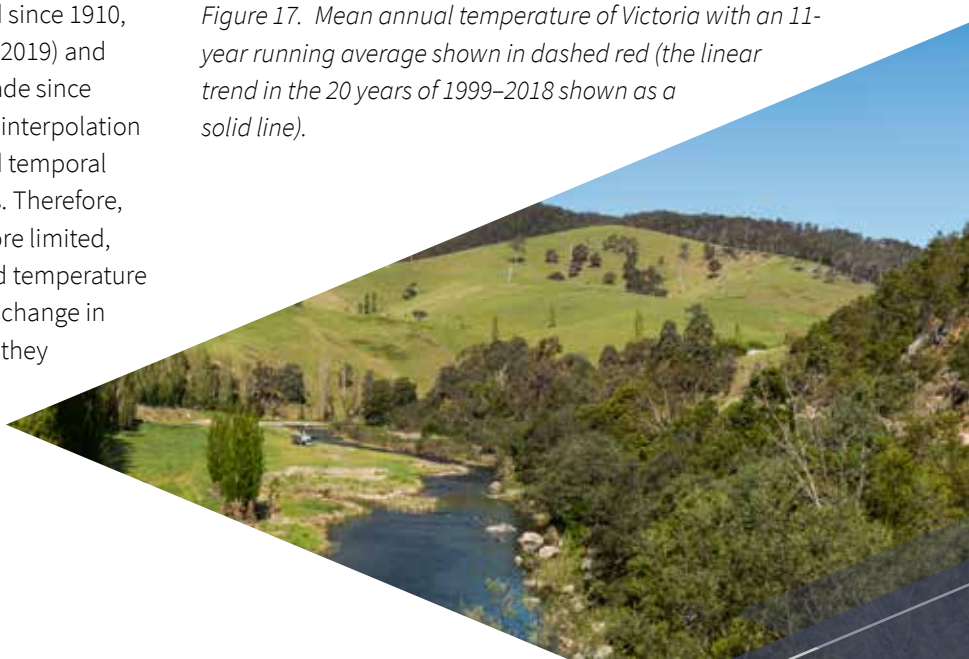

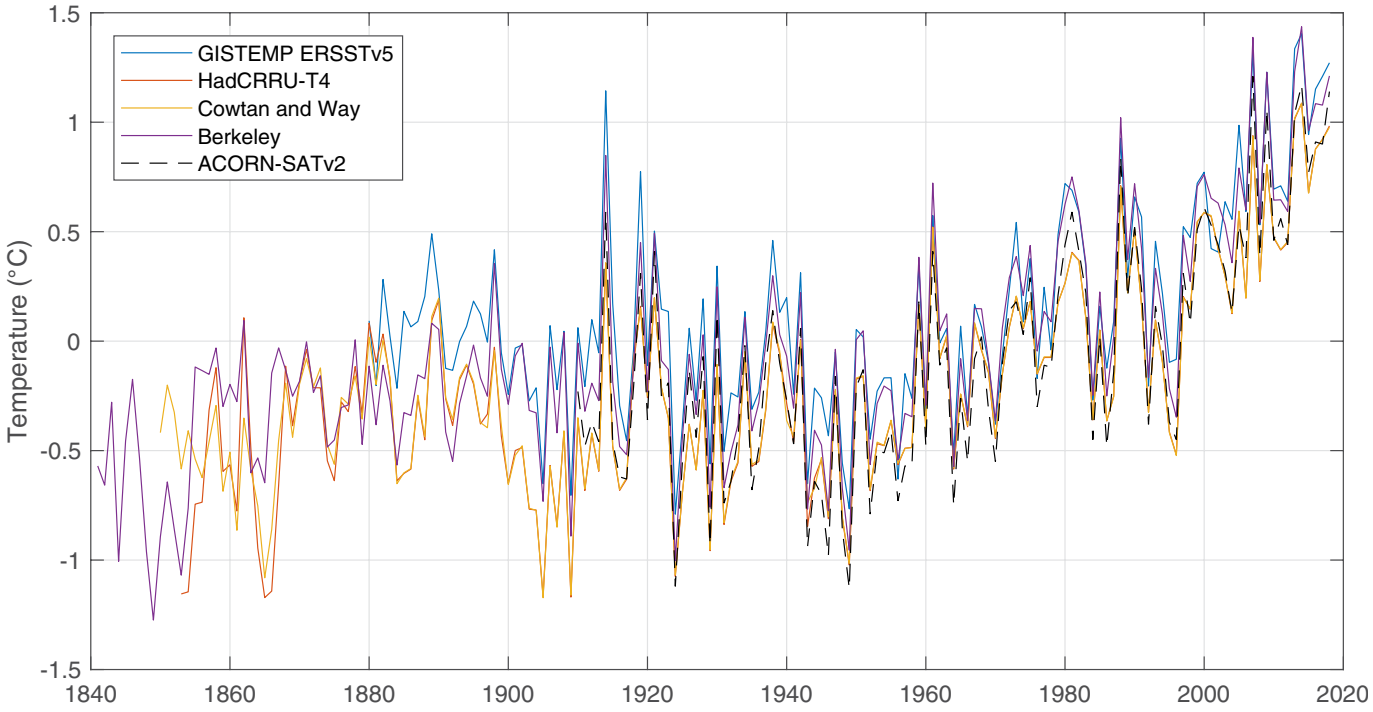

Figure 18. Mean temperature anomaly from 1961–1990 in Victoria in various gridded climate data sets: ACORN-SATv2 (dashed line), showing similar variability and very similar trends as the global temperature data sets kept internationally (GISTEMP, HadCRUT4, Cowtan and Way infilled HadCRUT4, Berkeley). Note that the global gridded data sets are generally on a coarse spatial grid, so Victorian temperature is often derived from a small number of grid cells, explaining some differences in the values for year-to-year variability. Also note there are much larger uncertainties prior to 1910, so the series presented here should be viewed with lower confidence.

5.2.2 Near-term temperature change (current to 2030)

The effect of all emissions scenarios is similar by 2030, so they are examined together. Under all plausible scenarios of greenhouse gas emissions (that is, scenarios ranging from ongoing high greenhouse gas emissions through to ambitious mitigation that could mean the world meets the Paris Agreement targets), the projected change in mean annual temperature between 1986–2005 and 2020–2039 is 0.5 to 1.3°C which is broadly consistent in both the CMIP5 global climate models and the VCP19 high-resolution simulations.

As shown in Figure 19 (and conceptually in Figure 4), these projected change values are the difference between the 20-year period 1986–2005 (centred on 1995) and the period 2020–2039 (centred on 2030). Using the recent trend found above (0.32°C/decade) as a guide, we are currently tracking within this projected range at the higher end but change over the relatively short period 1995–2018 is affected by natural variability and is not expected to stay constant until 2030. While the effect of a warming climate is persistently increasing the odds of hotter years and a positive (increasing) trend in temperature in the long-term, the effect of climate variability is still very important. The temperature trend for 2019–2030 will be influenced by processes of climate variability from year to year and decade to decade (such as the El Niño Southern Oscillation and related processes in the Pacific Ocean). Importantly, not every year will be warmer than the last, and natural variability could create a negligible or even negative trend over this shorter-term timeframe of 11 years, or conversely there could be periods of warming at a greater rate than the long-term trend. Taking model simulations as a guide to the theoretical pattern of warming in Victoria due to greenhouse gases, including the full range of potential climate variability, the linear trend in temperature in 2019–2030 is -0.8 to +1.3°C (median +0.3°C). This suggests that for climate warming and the full range of natural variability, a positive trend is likely, but a negative trend is possible over this short timeframe, or a much higher rate of warming than the long-term trend. Examples of two simulations that show a cooling or rapid warming over this period are shown as a red line in Figure 20. However, this does not account for the actual variability we have had in the observed world and given that we are tracking in the upper range of projections and have not been recently in a period of warming lower than the long-term trend, the possibility of

a rapid warming appears less likely than other possibilities. The prospect of narrowing this estimate by exploiting any predictability in the climate system is known as multi-year to decadal prediction and is a current area of active research (e.g. see the UK MetOffice website for more information https://www.metoffice.gov.uk/research/climate/seasonal-to-decadal and for the latest experimental forecasts done around the world: https://www.metoffice.gov.uk/research/climate/seasonal-to-decadal/long-range/wmolc-adcp).

Ongoing warming of the climate, including the average annual temperature of Victoria is given with *very high confidence*, as there is evidence from physical theory, process understanding, acceptable model evaluation, agreement of models with past trends and model agreement. Natural variability of the climate means that this long-term warming of the system may not be clear over short timeframes at the scale of Victoria.

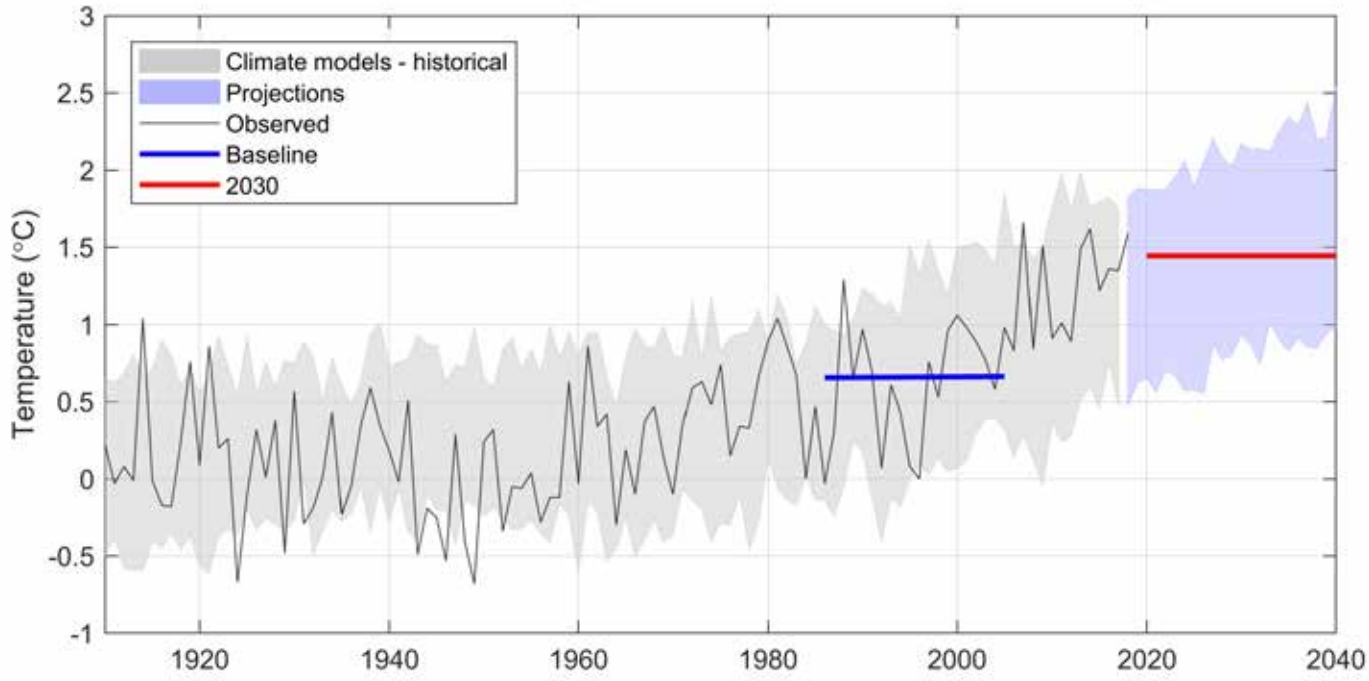

Figure 19. Victorian average annual temperature in observations and global climate model simulations relative to the pre-industrial era (all RCPs are examined together), showing the range among models. Blue and red lines show the average during the 1986–2005 baseline and 2020–2039 projected periods, respectively.

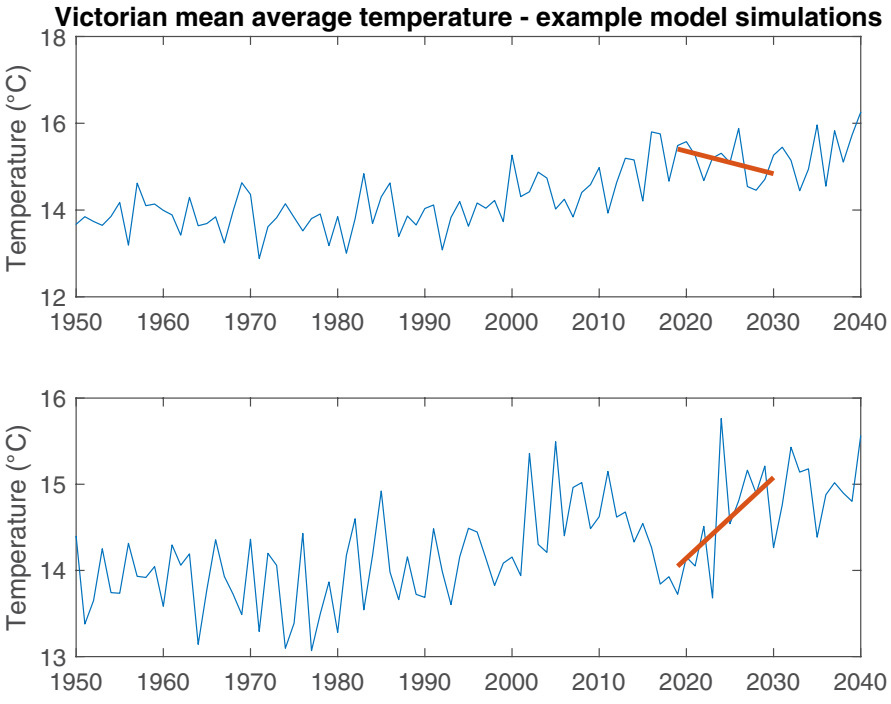

Figure 20. Example time-series from two GCM under RCP8.5 showing how a negative linear trend in temperature (red line; 2019–2030) can occur despite a warming climate, or how the warming may be more rapid than the long-term trend for this short window.

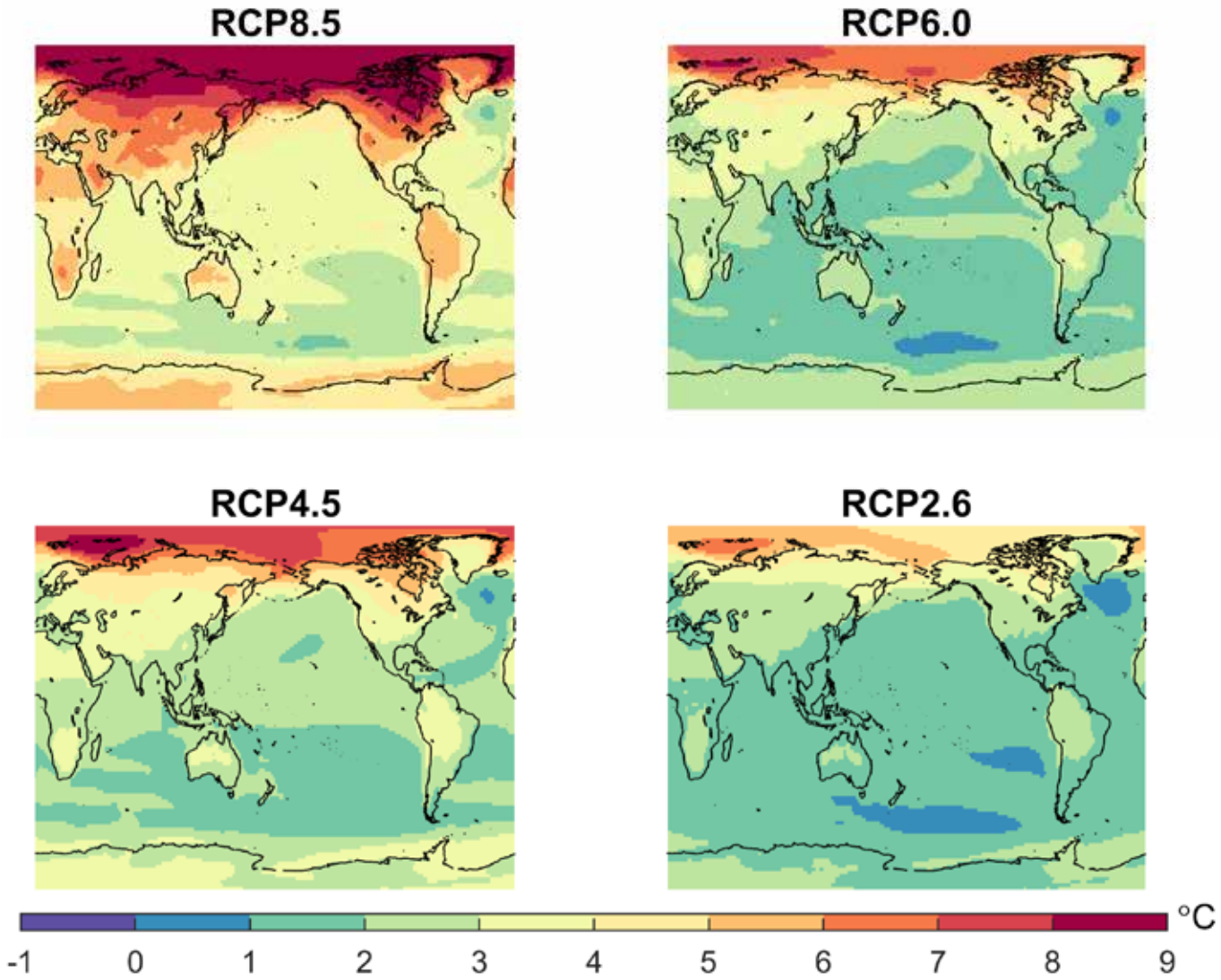

Figure 21. Model average projected change in near-surface (2 m) temperature between 1850–1900 (approximating the pre-industrial baseline) and 2080–2099 from all CMIP5 models under all four RCPs (including the two focused on in VCP19 RCP4.5 and RCP8.5).

5.2.3 Temperature change for this century

There are some general features of projected change in temperature that are relevant no matter which greenhouse gas emissions scenario we follow. These spatial patterns can be seen in the projected change under the two RCPs primarily used in this report, RCP4.5 and RCP8.5, as well as the other two RCPs that exist: a very low scenario RCP2.6, and a high scenario RCP6.0. The land regions are projected to warm more than the oceans, and the Arctic is a hot-spot of warming (Figure 21). The Southern Ocean and north Atlantic are areas of lower warming at this time scale. Australia is near the global average, and Victoria is also close to the global average.

The magnitude of warming later in the century depends strongly on the greenhouse gas emissions scenario the world follows. For a given emissions scenario, there is also a range of plausible changes given by the models. For Victoria as a whole, the projected temperature change between 1986 and 2005 and future periods centred on 2030, 2050 and 2070 show a growing difference between the highest RCP8.5 and the very low RCP2.6 (Figure 22). By 2080–2099, the range of change is 0.5 to 1.5°C for RCP2.6, through to 2.8 to 4.3°C under RCP8.5. These changes can be visualised as time-series (Figure 23) and bar plots (Figure 24). Both styles of plot show how the difference between RCPs grows as time progresses. The range among models (as an estimate of the range of climate response) also widens through the century. The very low scenario RCP2.6 is shown here for context, but the focus for projections in general is on the Paris Agreement target rather than RCP2.6 (see next chapter).

An ongoing warming of the climate is given with *very high confidence*, and the ranges of projected change are given with *high confidence*. Confidence is lower for the magnitude than the direction, as it is possible that processes such as climate feedbacks in future may respond outside the range of models due to processes that are currently unclear or poorly understood, creating either a higher or lower projection.

Temperature projections from the pre-industrial period out to 2100 from an example model that is in the mid-range of the models can be visualised using climate stripes (Figure 25). This shows that no future years are projected to be less than the pre-industrial temperature for the rest of the century, and under the higher emissions scenarios beyond around 2050 many years are projected to be above the maximum equivalent threshold for 2°C global warming since pre-industrial set by the Paris Agreement.

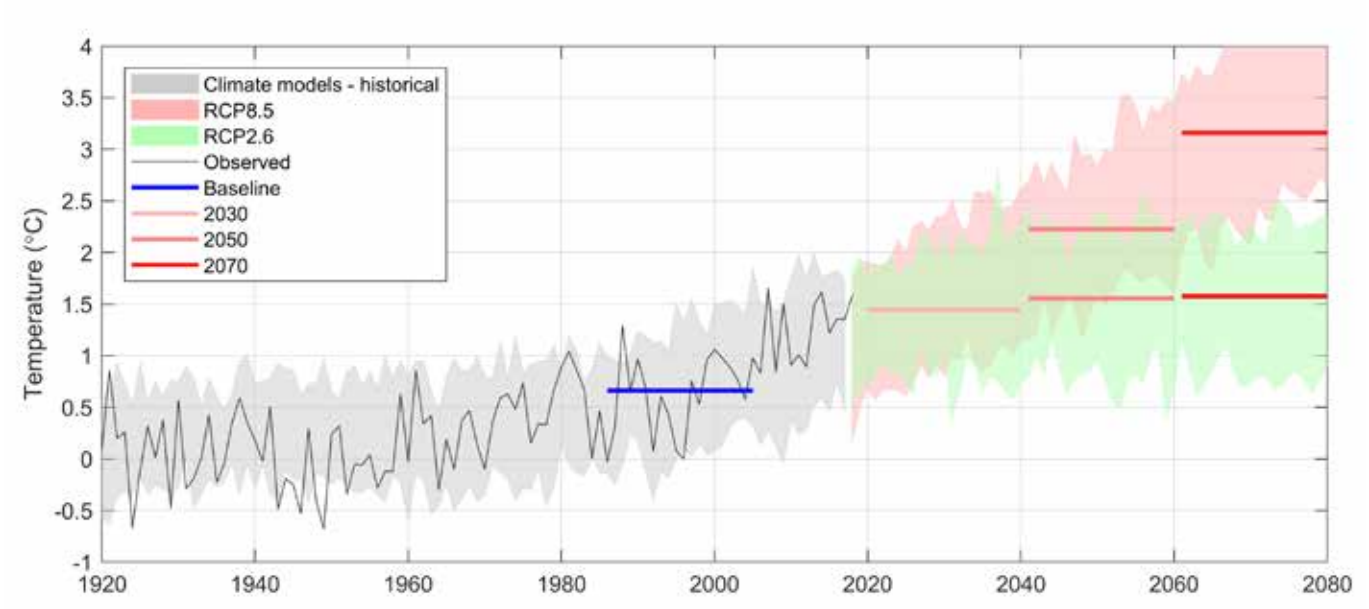

Figure 22. Average annual temperature of Victoria in observations and models relative to pre-industrial era, but in contrast to Figure 19 this plot extends the series to 2080 and shows the highest emissions pathway (RCP8.5) and the lowest (RCP2.6) separately, blue and red lines show the 20-year average temperature from the average of all models for each time period.

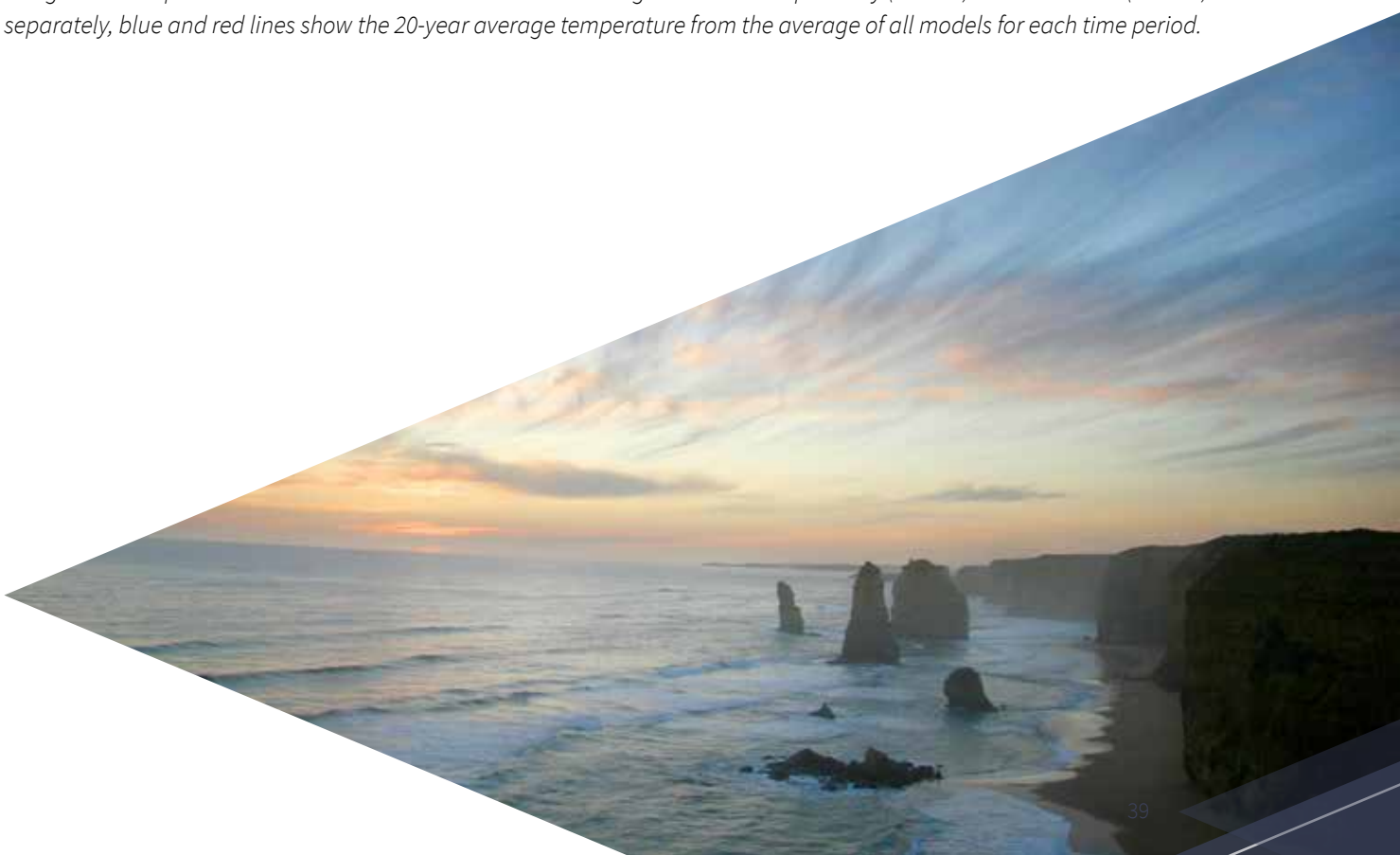

Presentation of area-averaged results

Time-series plots and bar plots both illustrate projected climate change and how the simulated change relates to the current climate.

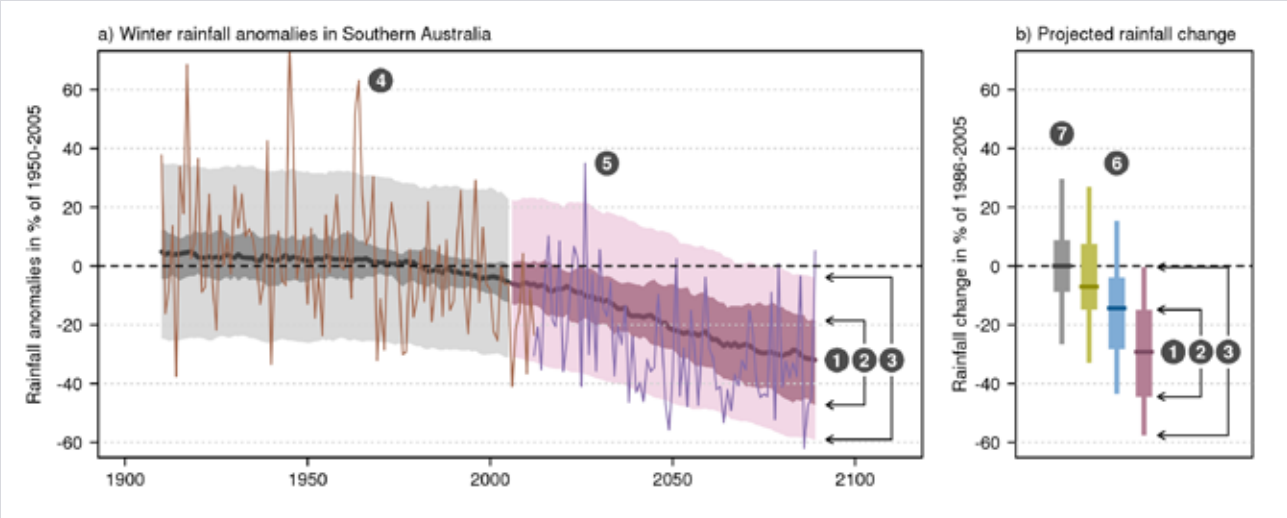

Figure B1. (a) Time series of observed and simulated change and (b) projected change according to different scenarios for winter (JJA) rainfall in southern Australia. Please note the different reference periods used in a and b. For explanations regarding the key elements see text below.

Time-series plots: the range of model results is summarised using the median (1) and 10th to 90th percentile range of the projected change (2) in all available CMIP5 simulations. The change in mean climate is shown as 20-year moving averages (Figure B1(a)). Dark shading (2) indicates the 10th to 90th percentile range for 20-year averages, while light shading (3) indicates change in the 10th to 90th percentile for individual years. Where available, an observed time-series (4) is overlaid to enable comparison between observed variability and simulated model spread. When CMIP5 simulations reliably capture the observed variability, the overlaid observations should fall outside the light-shaded range in about 20 per cent of the years. To illustrate one possible future time-series and the role of year-to-year variability, the time-series of one model simulation is superimposed onto the band representing the model spread (5). Note the 20-year running average series is plotted only from 1910 to 2090.

Bar plots: similar to time-series plots, bar plots also summarise model results using the median (1) and 10th to 90th percentile range of the projected change (2) in all available CMIP5 simulations. The extent of bars (2) indicates the 10th to 90th percentile range for difference in 20-year averages (reference period to a future period), while line segments (3) indicate change in the 20-year average of the 10th and 90th percentile, as calculated from individual years. The projection bar plots enable comparison of model responses to different RCPs (6), where RCP2.6 is green, RCP4.5 is blue and RCP8.5 is purple (Figure B1(b)). The range of natural internal variability without changes in the concentration of atmospheric greenhouse gases and aerosols as prescribed by the RCP scenarios is shown in grey (7). This range is estimated from the spread in projections for the period 2080–99 among simulations differing only in their initial conditions. In the above case, the median projection in all RCPs is for a decrease in winter rainfall. The models agree well on the magnitude of the decrease and therefore the spread in projected changes (coloured bars) is only slightly larger than due to natural internal variability alone (grey bar). In cases where the models do not agree on the magnitude and/or sign of the projected change, the range of projections is much larger than that due to natural internal variability.

Source: CSIRO and Bureau of Meteorology 2015

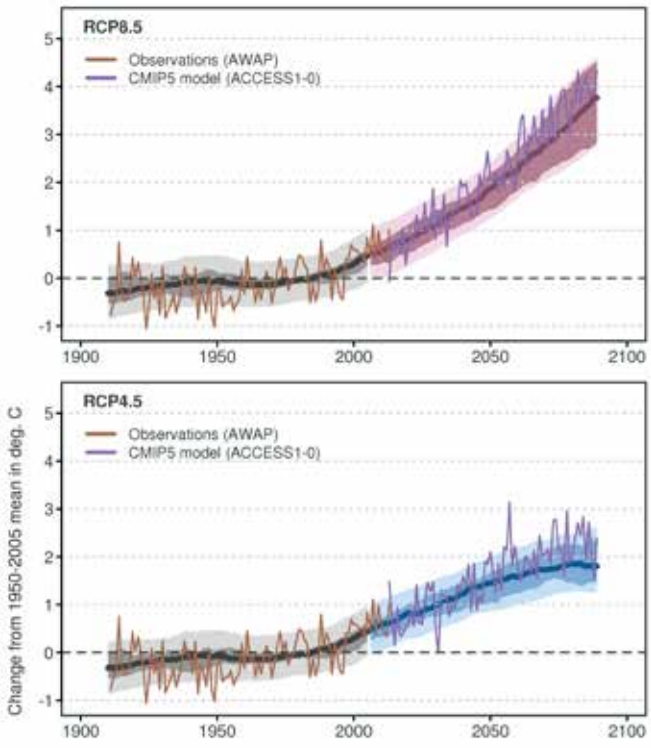

Figure 23. Time series of modelled 20th and 21st century mean annual temperature for Victoria, relative to 1950–2005 for RCP4.5 and RCP8.5 from CMIP5 GCMs. Observed annual temperatures (brown line) and an example model series (purple line) are included on each graph to illustrate variability and change (observed and simulated). For a guide to understanding these graphs, see the box on page 40. Note a different, longer baseline is used here than elsewhere to more clearly illustrate the long-term context of change.

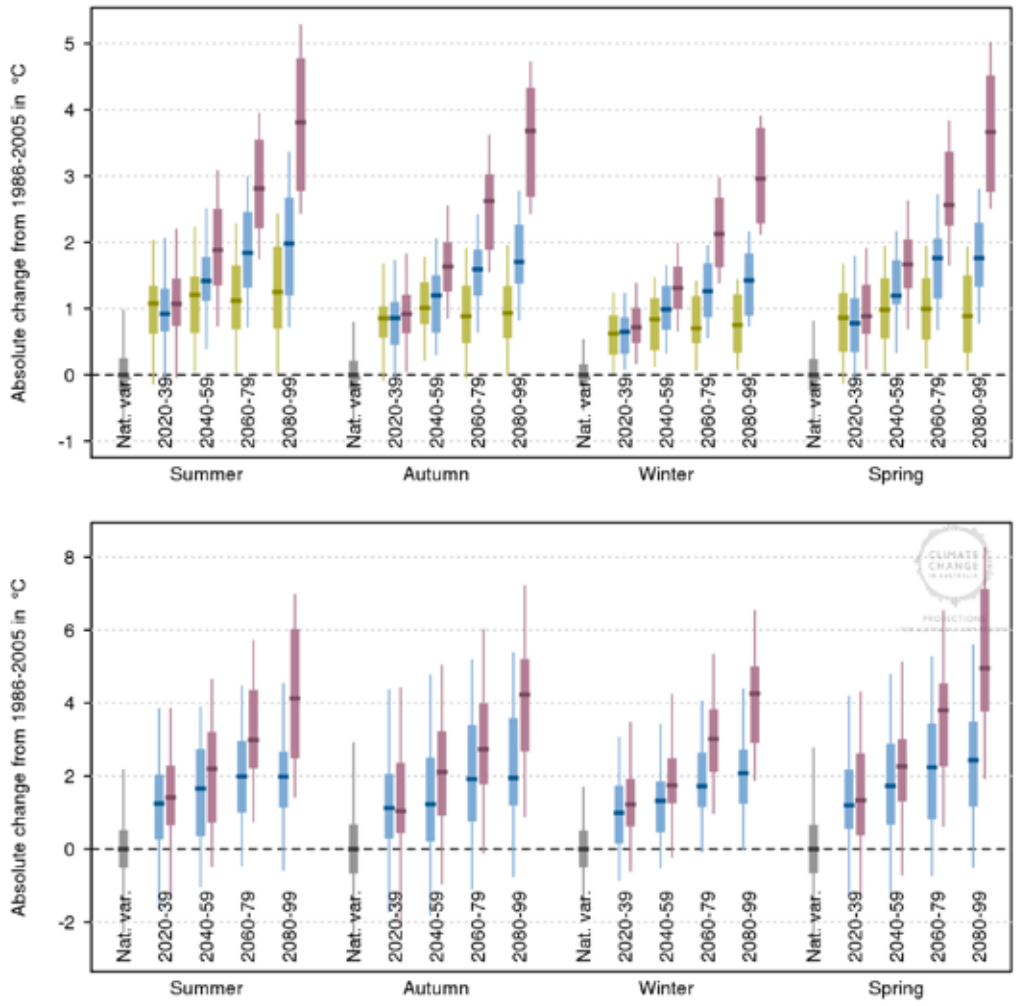

Figure 24. Bar plot of projected change in mean temperature for four future time-periods, relative to 1986–2005 for Victoria. The top panel shows results from 40 CMIP5 GCMs and the bottom: the results from six CCAM simulations for RCP4.5 and RCP8.5. Grey is natural variability only, green is RCP2.6, blue is RCP4.5 and red is RCP8.5. Thick bars show the range of 20-year averages from all models; the dark line shows the median of model results; the thin bar shows the temperature range that year-to-year variability can contribute on top of the longer-term variability and change. For a guide to reading this graph, see the box on page 40.

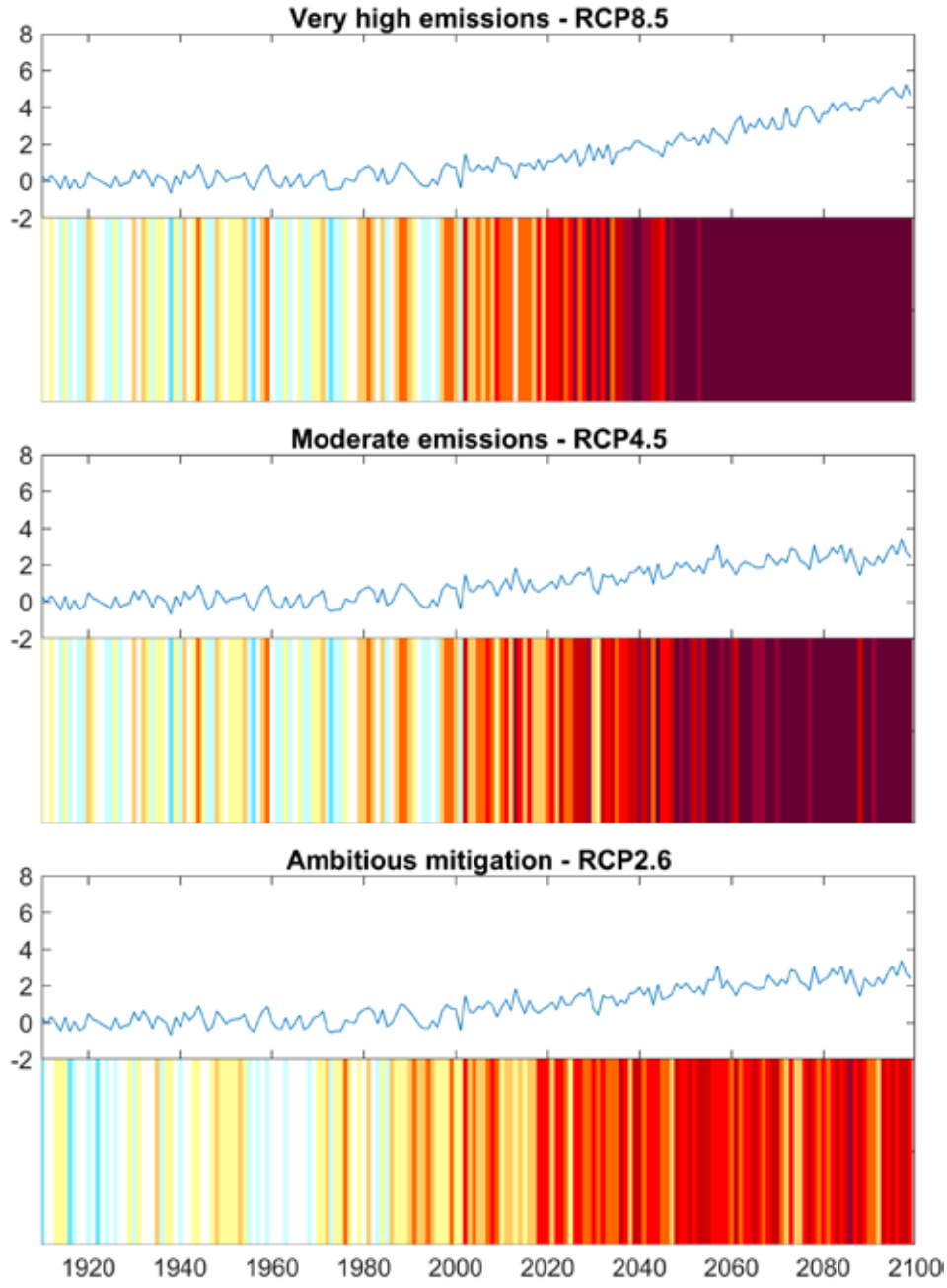

Figure 25. Example series of Victorian average annual temperature relative to 1850–1900 approximating pre-industrial times from a single climate model simulation. The plots include climate stripes as in Figure 1, but the colour scale is different in Figure 1, and tops out at 2.3°C, the higher estimate of what Victoria's temperature could be at 2°C global warming.

The high-resolution CCAM simulations show a similar range of changes to those from the entire CMIP5 set of simulations, with a few important cases where the upper range of change is higher in CCAM than in GCMs (Table 6). For average annual temperature, most differences in the upper range are less than 0.5°C, but there is one case of 0.7°C by the 2090s (RCP4.5). There are greater differences in some seasons than others (Table 7), where the CCAM simulations show much higher values in spring than the GCMs (up to 1.2°C). The lower bound of the 10th to 90th percentile range is similar in CCAM as the GCMs in all time periods, RCPs and seasons: all within 0.5°C with one exception (0.7°C in spring in RCP4.5).

There are a number of plausible physical explanations for the difference in the upper estimate of projected warming in CCAM compared to GCMs. The strongest case is where the CCAM projection is drier and hotter than the GCMs for spring. This is plausible since a drier climate is typically associated with warmer temperatures. In addition, the higher-resolution simulation of the response of the land surface to lower rainfall in CCAM could be contributing to warmer temperatures. Confidence in the added value from CCAM compared to the GCMs is given with *medium to high confidence*, as the model evaluation of CCAM was acceptable and there appears to be a physical explanation for the higher values. Therefore, we present a higher hot case for projected change, but this should be used along with the full range of other possibilities, and not used to the exclusion of other inputs.

A plausible hotter 'hot case' projection

The high end of projected change is higher in the new simulations than in the GCMs, by up to 0.5°C in the state average, and up to 1°C in some regions.

Possible reason: enhanced response of land surface to drying compared to low resolution models

Seasons: especially spring and summer

Regions: all regions, but especially in the Gippsland, Grampians and Hume regions (the central and southeast of Victoria)

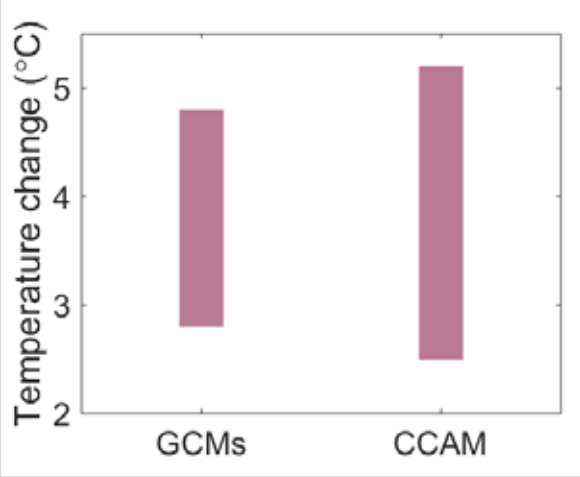

Range of change in summer temperature in 2090 under high emissions (RCP8.5) from the models used as input and the high-resolution downscaling

Table 6. Projected changes to Victorian average annual temperature relative to the 1986–2005 baseline in GCM and CCAM simulations (10th to 90th percentile range of 20-year running average in each period)

	RCP2.6	RCP4.5	RCP8.5
2030 (2020–2039)	GCM: 0.55 to 1.0°C	GCM: 0.6 to 1.0°C CCAM: 0.8 to 1.0°C	GCM: 0.7 to 1.2°C CCAM: 0.9 to 1.3°C
2050 (2040–2059)	GCM: 0.61 to 1.3°C	GCM: 0.85 to 1.5°C CCAM: 0.9 to 1.8°C	GCM: 1.3 to 2.0°C CCAM: 1.4 to 2.4°C
2070 (2060–2079)	GCM: 0.49 to 1.3°C	GCM: 1.3 to 1.9°C CCAM: 1.4 to 2.1°C	GCM: 2.1 to 3.1°C CCAM: 2.2 to 3.5°C
2090 (2080–2099)	GCM: 0.48 to 1.5°C	GCM: 1.3 to 2.2°C CCAM: 1.6 to 2.9°C	GCM: 2.8 to 4.3°C CCAM: 2.6 to 4.7°C

Table 7. Projected change to seasonal temperature around 2090 (2080–2099) relative to the 1986–2005 baseline for each calendar season (e.g. summer is December to February)

	RCP2.6	RCP4.5	RCP8.5
Summer	GCM: 0.7 to 1.9°C	GCM: 1.2 to 2.7°C CCAM: 1.7 to 3.2°C	GCM: 2.8 to 4.8°C CCAM: 2.6 to 5.3°C
Autumn	GCM: 0.55 to 1.3°C	GCM: 1.4 to 2.3°C CCAM: 1.7 to 2.3°C	GCM: 2.7 to 4.3°C CCAM: 2.9 to 4.8°C
Winter	GCM: 0.33 to 1.2°C	GCM: 0.9 to 1.8°C CCAM: 1.2 to 2.5°C	GCM: 2.3 to 3.7°C CCAM: 2.3 to 3.7°C
Spring	GCM: 0.34 to 1.5°C	GCM: 1.3 to 2.3°C CCAM: 2.0 to 3.5°C	GCM: 2.8 to 4.5°C CCAM: 2.8 to 5.6°C

5.2.4 Temperature extremes

The new projections show increases in daily maximum and minimum temperatures that are consistent with hotter and more frequent hot days, fewer cold days, more frequent and more intense heatwaves, as well as fewer extreme cold nights.

Temperature-related impacts come from the change in background average temperature as well as the incidence of extremes, either high or low. For some applications, the extremes have more impact than the average. Examples include hot extremes that cause damage to infrastructure and result in heat stress among vulnerable people. But for other applications like agricultural growing conditions, the entire temperature regime is important, that is, the average and the extremes (Harris et al. 2018).

Climate extremes are by definition rare events, so accurately characterising their frequency and intensity is difficult and highly dependent on having a very long climate record. The longer the record, the more 'signal' (extreme events) there will be relative to the 'noise' of the more common everyday events. As Victoria's climate record is just over 100 years in duration, events with say a 1-in-20-year occurrence on average (recurrence interval) are expected to have occurred only five or so times in the entire record. For this reason, it is not appropriate to calculate simple statistics of the observed or simulated extreme events as is done for averages. Instead, extreme distribution fitting and other statistical techniques are used.[3] Here the changes to annual maximum (the average 'hottest day of the year' over a 20-year period) and the 20-year average recurrence interval (ARI20) have been calculated by fitting statistical distributions to the climate data. An ARI20 is expected to be met once every 20 years on average with a randomness on top of this average value, as it is not met regularly every 20 years. Another way of thinking of an ARI20, is that there is a 5% chance of it occurring in any year.

An increase in the average temperature leads to a corresponding increase in hot extreme daily maximum temperatures and a decrease in cold extreme daily minimum temperatures, assuming no change to variability or timing of events. Therefore, the broad framing of changes to extreme temperatures follows directly from the changes to averages in the previous section – changes are projected under all scenarios, with greater change for higher emissions scenarios and further timeframes. The predicted hotter and more frequent hot days, fewer cold days, more intense heatwaves and fewer extreme cold nights is the most important and relevant message from the projections and is given with *very high confidence*. But within this general framework, there is great interest in the possibility that extremes might change in ways that are different from those expected from the change in the average. This could be due to a change in the nature or timing of the events that bring extremes.

In certain circumstances, we expect the increase in heat extremes such as the ARI20 to increase more or less than the increase in the average. In particular, heat extremes can be amplified by soil moisture–temperature feedbacks, where less rainfall and less evaporative cooling allows hotter temperatures (Seneviratne et al. 2010; Seneviratne et al. 2012). Victoria as a whole is projected to get drier, especially in spring where hot, dry conditions set up a dry landscape for summer heatwaves. Also, the land–sea contrast may change in Australia, meaning greater heat extremes over land compared to over ocean due to changes in the movement of heat from warmer continental interiors (Watterson 2008). A recent example of where heat over land was not dispersed quickly is during the summer of 2018–19 where long hot spells were experienced in many inland locations. The national climate projections (CSIRO and Bureau of Meteorology 2015) indicate that in most regions of Australia, extreme daily maxima are projected to change by a similar amount as the average, but with a few important regional exceptions. Exceptions include southern Victoria, where the extremes projections have a hotter hot end. For example, in the Southern Slopes Victoria West region under RCP8.5 by 2090, the annual average daily maximum temperature is projected to increase by 2.4 to 4.2°C. However, the annual maximum range is 2.5 to 5.8°C and the ARI20 is 2.9 to 6.3°C. This means that the average daily maximum temperature is projected to increase from the value in 1986–2005 (14.3°C) to as much as 18.5°C. In contrast, the annual maximum could increase from 36°C in 1986–2005 to 41.8°C around 2090. The results are different for daily minimum temperature, where the projected changes are similar for the average and extremes, with only small differences for the top of the range.

3 See https://www.climatechangeinaustralia.gov.au/en/climate-campus/climate-extremes/ for details on extremes and analysis methods

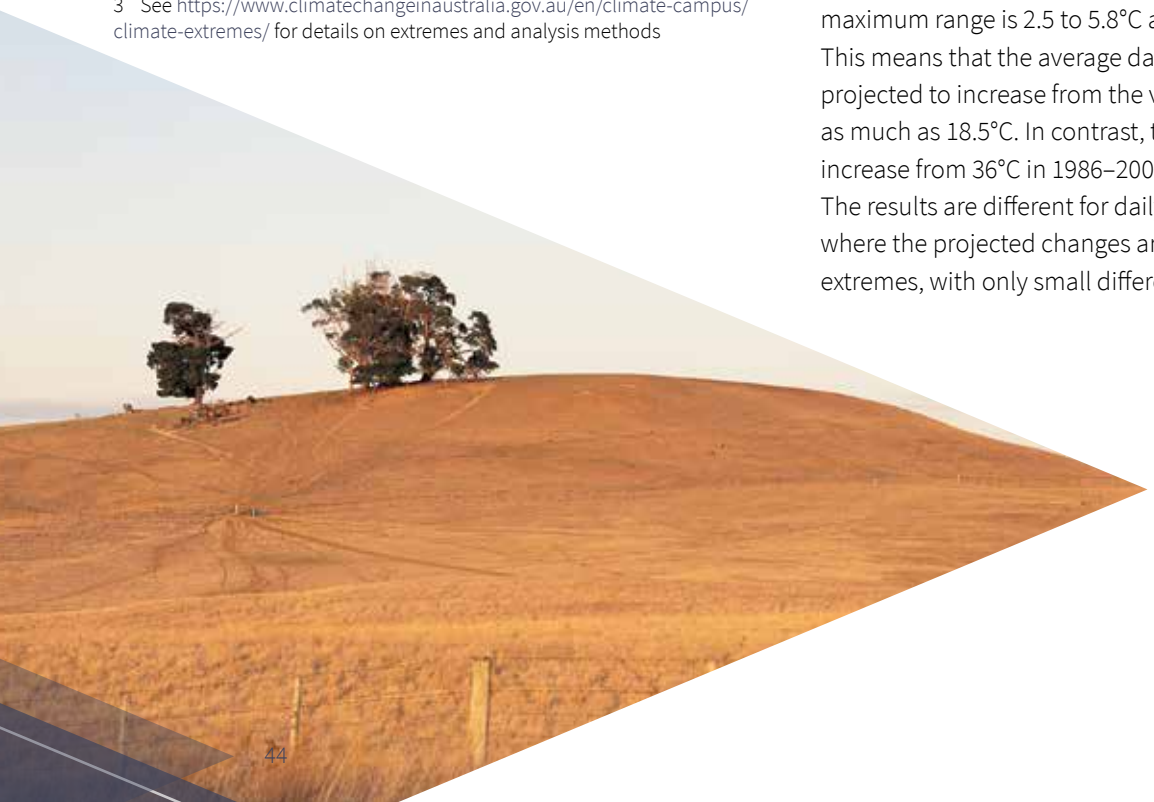

A plausible projection of hotter heat extremes

Much hotter upper end of projected increase in heat extremes than GCMs projected.

Possible reason: as for mean temperature (response to drier climate, resolution of coasts etc.)

Seasons: especially winter, but also spring and other seasons

Regions: all

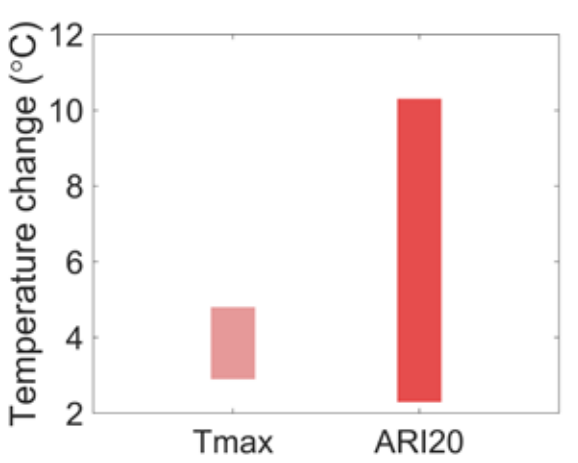

Range of change in winter Tmax and ARI20 in 2090 under high emissions (RCP8.5) in Gippsland from the VCP19 simulations

High-resolution CCAM climate simulations developed for VCP19 show a drier rainfall projection than the host models in some regions and seasons, and the response of the land and vegetation to a drier environment is better simulated in VCP19 runs than in GCMs. Also, the land–sea contrast near the coast is better resolved and simulated in VCP19 runs than in GCMs, where GCMs resolves the coast as a few large boxes, whereas CCAM has many cells to simulate the effects of the coast. Changes in extreme temperatures show a strong land–sea contrast with much larger increases over land than ocean. A land–sea contrast is found in all projections, but the difference is more highly resolved in VCP19 runs than in coarser resolution models. These factors are among the likely drivers of differences between the CCAM VCP19 simulations and the host GCMs and suggest the added resolution of CCAM downscaling for VCP19 has potentially produced a more realistic simulation of temperature response. Similar to the GCMs, VCP19 projects a change in both annual maximum and 20-year extreme temperatures with a higher hot end than for average daily maximum temperature in the coastal and metropolitan regions such as Barwon, but not in inland regions such as Mallee (Figure 26 where the 10 high-resolution VCP19 regions are shown using their codes from Table 4). This is consistent with the CCIA projections and previous findings, where coastal sub-clusters in southern Victoria showed a stronger enhancement than Murray Basin (CSIRO and Bureau of Meteorology 2015). Notably, the GCMs show a larger increase in ARI20 compared to daily maximum temperatures than the VCP19 runs do. However, striking changes are projected seasonally, with a huge enhancement of daily maximum temperature extremes compared to the change in the average for winter and spring. For example, in the Greater Melbourne region projections for daily maximum temperature in winter by 2090 under RCP8.5 are 2.7 to 4.2°C, but the projection of ARI20 maximum temperatures is 2.3 to 10.0°C. This extreme hot end appears in a single model simulation and for 2090 under high emissions. This model run is CCAM downscaled from HadGEM2-CC and shows extreme drying (by up to 45% in spring), contributing to a land–surface feedback driving hotter hot days. It is unclear if other downscaling methods would replicate this result for Australia at the time of writing, which would have helped determine the level of confidence in this projection. In the absence of additional downscaling results we consider this model simulation is extreme, but physically plausible so is presented as a worst-case scenario to be used in conjunction with the full range of results and scenarios.

The changes projected under high emissions for the far future are extreme compared to the climate we are used to. Under RCP8.5 by 2080–2099, the projections indicate that locations within Victoria could experience days over 55°C in summer, and days over 33°C in winter. An example of the daily maximum temperature in an extreme day in the 2050s for the model with the greatest drying and warming (HadGEM2-CC downscaled by CCAM for VCP19) is shown in Figure 27. Note that the temperatures for Gippsland in this example are elevated due to the temperature bias described in section 4.2.1.

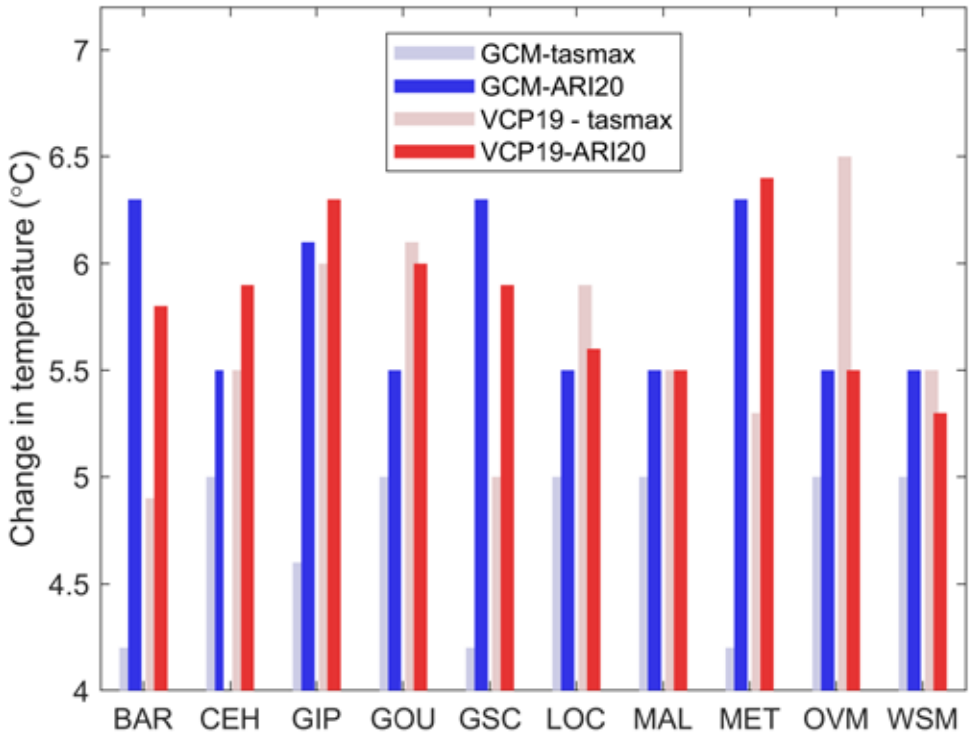

Figure 26. The upper range of projected annual daily maximum temperature change and the 20-year recurrence interval (ARI20) annually for RCP8.5 between 1986–2005 and 2080–2099 for each of the 10 VCP19 regions, the top of bars show the 90th percentile range from GCMs and the highest VCP19 run. The 10 high-resolution VCP19 regions are shown using their codes (see Table 4 for full names)

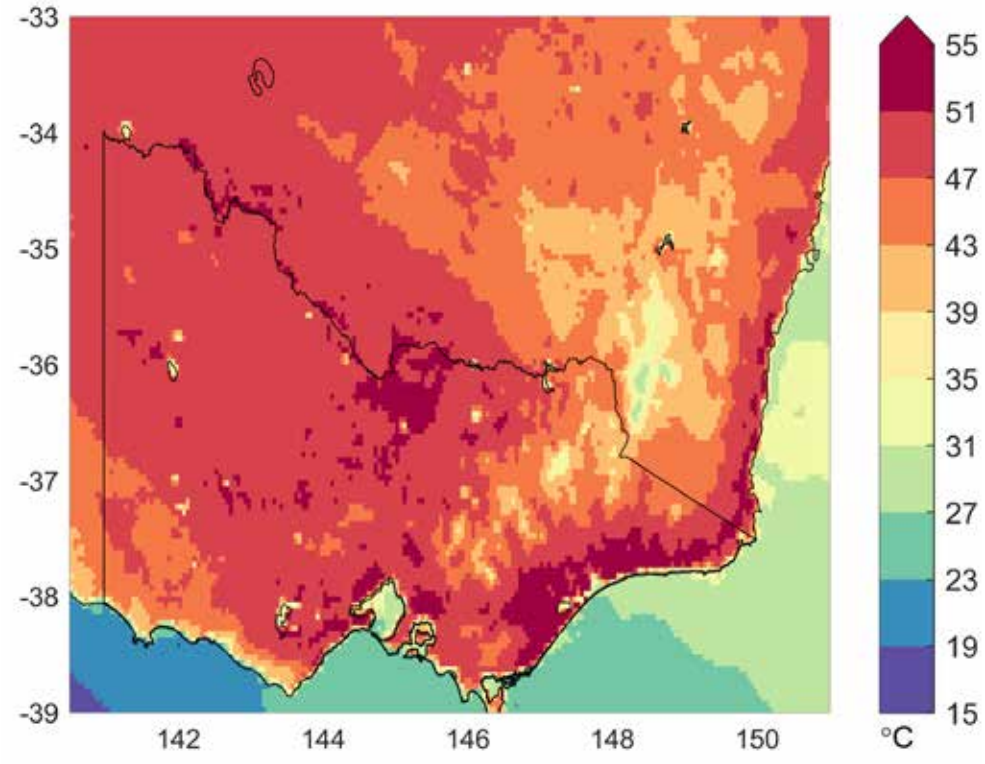

Figure 27. Daily maximum temperature for an example extreme heat day simulated under a very high scenario (RCP8.5, a summer day in the 2050s, HadGEM2-CC model downscaled by CCAM), where Melbourne reaches 50°C, and even higher temperatures inland. There is a warm bias in the simulation associated with the Gippsland region, so the temperature may be artificially elevated near the southeast coast. Note this is not the hottest day in simulations, it is just indicative of a very hot day in the future climate without a historical precedent.

In contrast to daily maximum temperatures, extremes of daily minimum temperature are lower than the change in average temperatures under a high emissions scenario and far future time scale. Dry conditions with clearer skies and less insulating effect of cloud cover are more conducive to heat loss from the Earth's surface and cold nights, so daily minimum temperatures and specifically the extreme minimums are cooler than if cloud and rainfall stayed the same. The effect on minimum temperatures is present in GCMs and in VCP19 runs and is particularly enhanced in inland regions such as the Mallee (Figure 28).

This effect is also relevant to frosts, where cold, clear nights are projected to persist longer than expected from a change in the average temperature would suggest. This is consistent with past trends, where frosts in some regions, particularly in spring, have in fact increased in frequency despite an increase in the average temperature (Crimp et al. 2016).

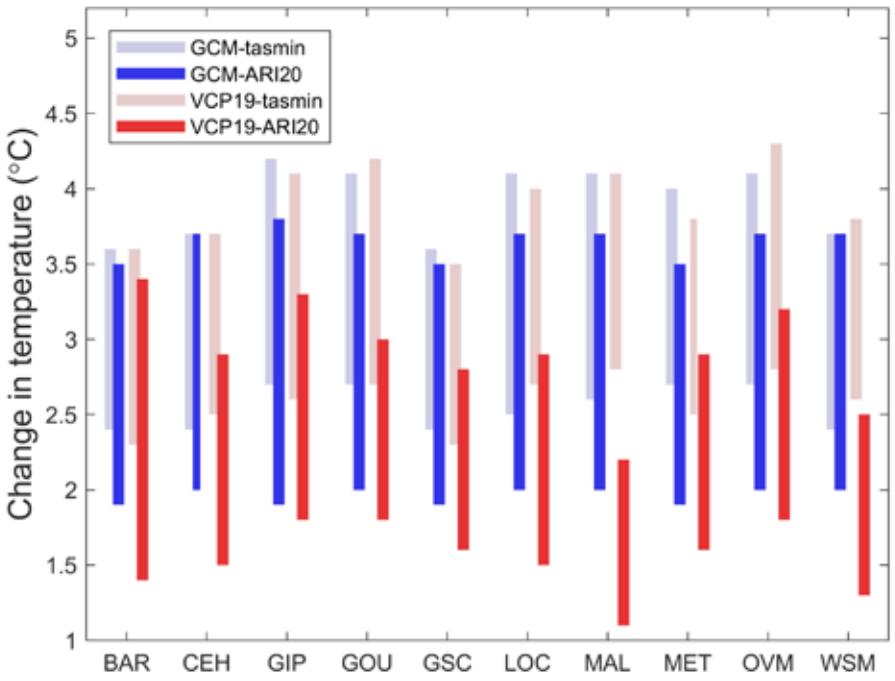

Figure 28. The upper range of projected daily minimum temperature change and the 20-year recurrence interval (ARI20) annually for RCP8.5 between 1986–2005 and 2080–2099 for each of the 10 VCP19 regions, the bars show the full model ranges.

5.3 Rainfall

Rainfall is one of the less certain projections but is of great interest to almost every sector of the Victorian community. Changes to the climate features described in Chapter 3 (e.g. atmospheric circulation) are the dominant drivers of changes to rainfall in this region, but with some influence from direct effects of a warmer climate (e.g. increased convection). Rainfall variability is high in Victoria, so any trend due to climate change is present amid much natural variability. This can be seen in the difference in the time-series of rainfall compared to temperature in past changes (Figure 29) and also for projected changes in future.

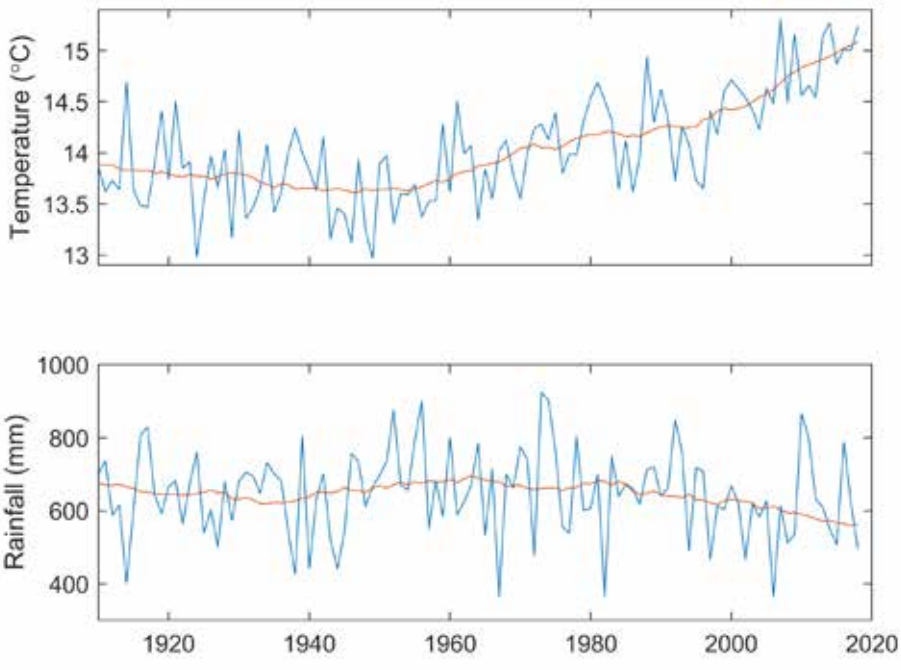

Figure 29. Victorian average annual temperature (top) and rainfall (bottom), showing the clearer trend compared to variability in temperature than in rainfall. Blue line is the annual values, red line is the 11-year running average.

5.3.1 Past changes

Using the Bureau of Meteorology's Australian Water Availability Project (AWAP) gridded climate data set of Jones et al. (2009), there has been a negative trend in rainfall in most seasons in recent decades (Figure 30). Trends are typically larger on the windward slopes of mountains or on the peaks; however, the mean rainfall is generally higher, so changes are not as notable as a proportion (%). Decreases are greater in the cooler seasons (Figure 31). Given that rainfall can have high variability from one decade to another (e.g. Figure 29), the start and end dates of any linear trend can have a strong influence on the result and should be carefully noted when comparing results.

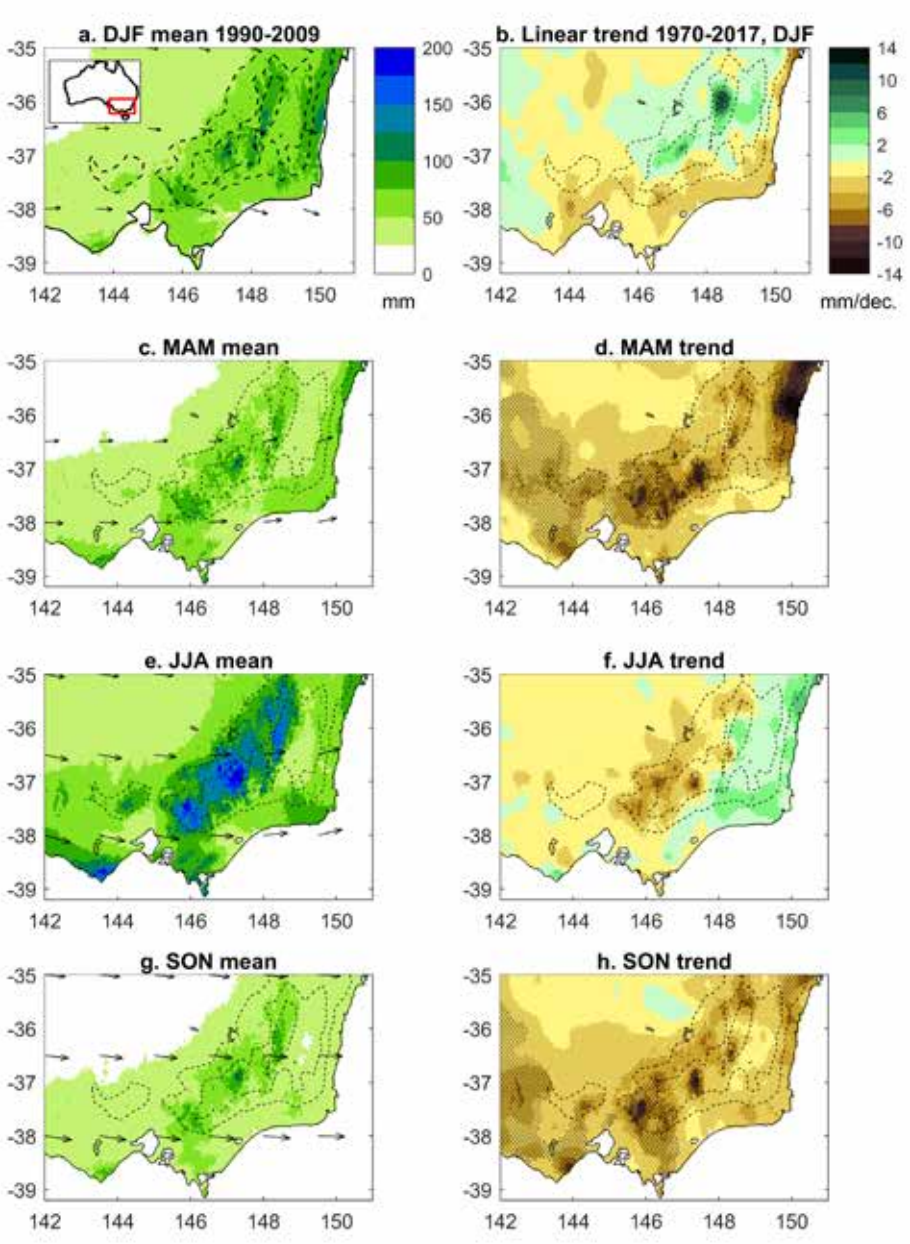

Figure 30. Rainfall mean and trends in the AWAP data set. (a) mean rainfall in 1990–2009 in summer (DJF), inset shows the location of the domain within Australia, vectors show the mean 850 hPa wind; (b) linear trend in mean rainfall in 1970–2017 (mm/decade) in DJF; (c) mean in autumn (MAM); (d) trend in MAM; (e) mean in winter (JJA); (f) trend in JJA; (g) mean in spring (SON); h) trend in SON. Dashed lines show topography at contours of 400 m, hatching shows statistical significance of the linear trend at the 0.1 level. (Source: Grose et al. 2019b)

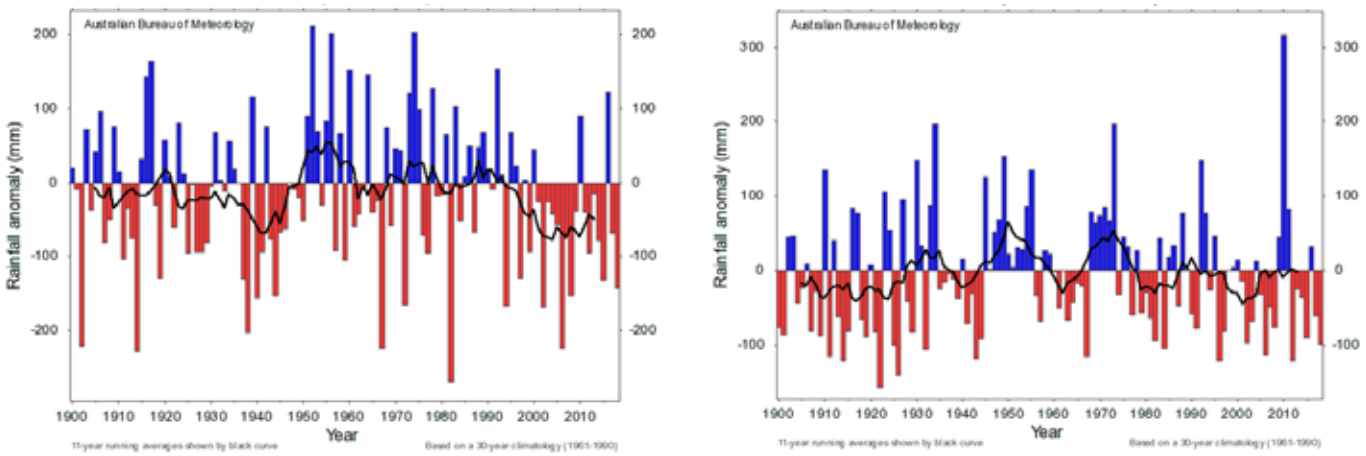

Figure 31. Time-series of Victorian average rainfall for April–October (southern wet season) and November–April (northern wet season) rainfall relative to the 1961–1990 average

5.3.2 Projected change – global and Australia

Globally-averaged rainfall is projected to increase as the atmosphere gets warmer. However, there is a large range of changes by region, with some areas projected to get wetter and others drier. There is good physical evidence and agreement between the most recent set of GCMs (CMIP5) for the mid-latitude regions of around 30–45°S to get drier – but with seasonal differences and differences between longitudes (Figure 32). There is high agreement for a decrease in rainfall across much of southern Australia in winter, particularly in the southwest. Victoria is located at the eastern edge of this projected change pattern. In summer, the region of projected rainfall decrease is to the south of Australia, and Victoria sits at a boundary between regions of projected increase and decrease, making it difficult to determine the projected change in summer specifically in Victoria.

Examining the broadscale changes over the Australian region in the GCMs, the 50 km CCAM simulations of VCP19 and various previous downscaling studies, we see how the model selection and downscaling steps modify the model mean projection of change (Figure 33). The mean of the six GCMs is broadly similar to the full set of GCMs for southeast Australia, although it shows some differences in other parts of Australia. VCP19 high-resolution simulations modify the mean signal of the six GCMs in a few ways. The projected change in northern Australian wet season (mainly DJF and MAM) is drier than the GCMs (results for JJA should be ignored as the change represents a percentage change on top of a very low rainfall amount in the north). VCP19 runs show an enhanced drying over southern Australia in several seasons, including Victoria (in section 5.3.3). Regional patterns linked to mountains and coastlines emerge (also covered in section 5.3.3). Notably, the VCP19 runs do not replicate the broadscale rainfall increase in DJF and MAM found in NRM-CCAM and NARCliM. In the case of CCAM there have been changes to the aerosol feedbacks, convection parameterisation and land-surface model which could account for some of these differences, although the exact reason for the change in the CCAM predictions is still under investigation.

Figure 32. Projected change in average rainfall (%) for the southern hemisphere in calendar seasons of summer (DJF) and winter (JJA) from 45 CMIP5 models between 1986–2005 and 2080–2099 under RCP8.5. Stipples indicate where 80% or more of models agree on the sign of change (i.e. more than 35 of the 45 models).

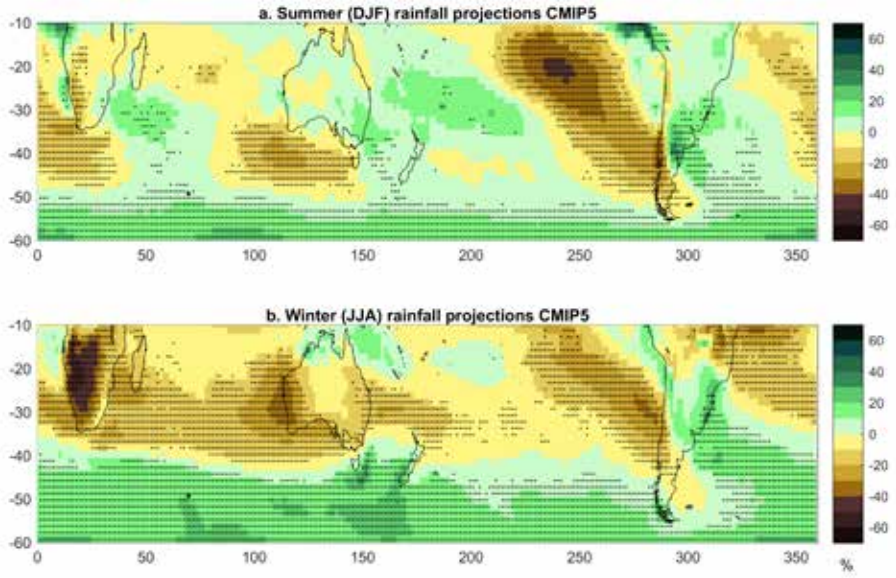

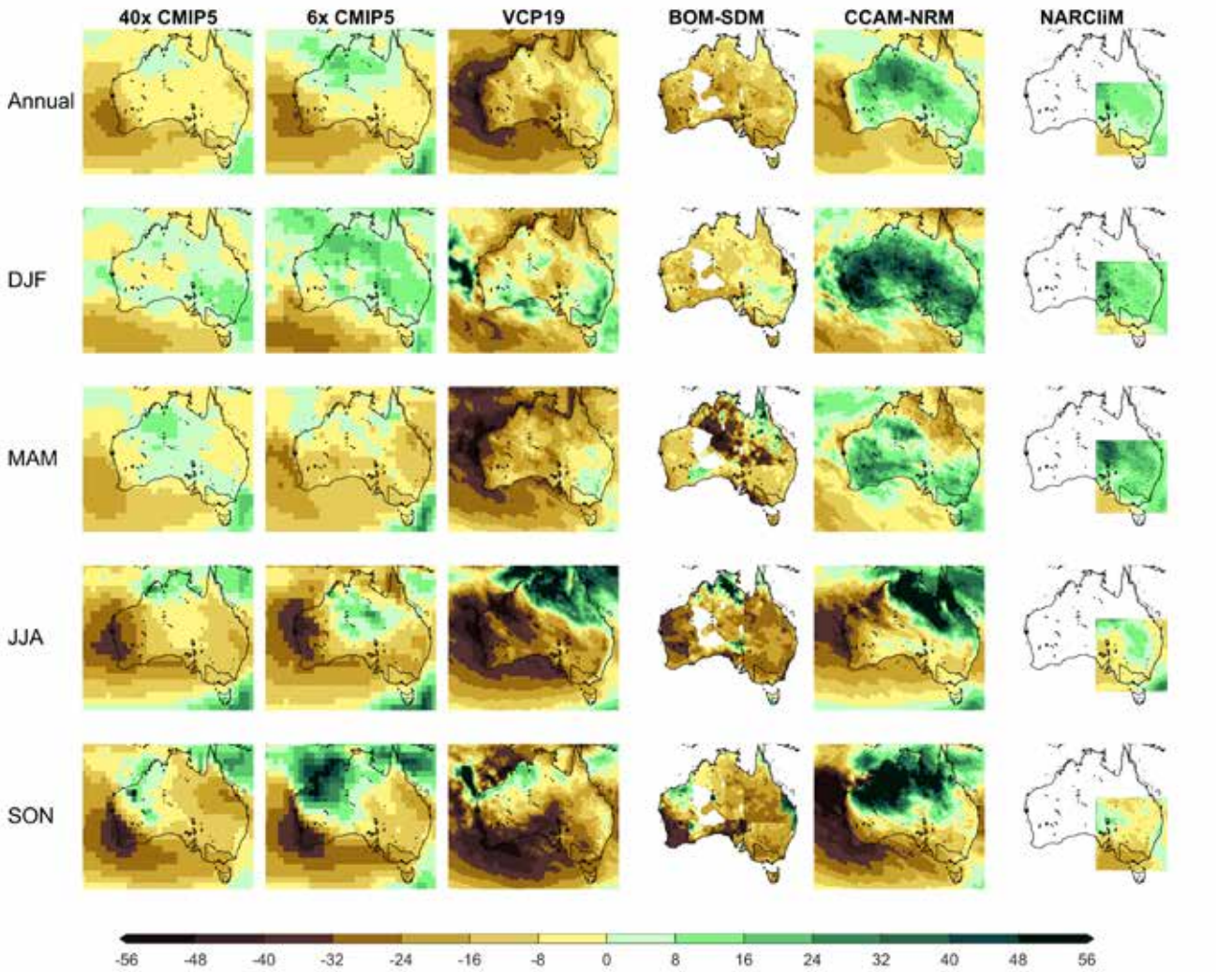

Figure 33. Model mean projected change (%) in average rainfall from different sets of model output: 40 CMIP5 models, the six CMIP5 models used as input to VCP19, the six new CCAM runs for VCP19 (50 km intermediate runs), 23 runs of the Bureau of Meteorology statistical downscaling model (BOM-SDM), six 50-km CCAM runs done previously for the NRM project, and 12 runs from the NARCLiM project. Change is shown for 1986–2005 to 2080–2099 under RCP8.5 except NARCLiM which shows 1990–2009 to 2070–2089 under SRES A2.

5.3.3 Projected change – Victoria and sub-regions

There is a range of projected change in average annual Victorian rainfall, but for the majority of CMIP5 GCMs (and hence, the model median) there is a projected decrease (Figure 34, left). The magnitude of the dry end of projections is greater under higher RCPs (compare RCP2.6 to RCP8.5). This is broadly replicated in the new CCAM simulations; however, the median of the six CCAM runs is lower than the GCMs for RCP8.5 by 2090 (Figure 34, right).

When broken down by season the projected decrease is larger, and with greater model agreement, for winter and spring. Changes are smaller, with less model agreement in summer and autumn (Figure 35), again with broad agreement between the CMIP5 GCMs and the new CCAM simulations. Specific differences include the median magnitude of change by late in the century under high emissions – consistently drier in CCAM than CMIP5.

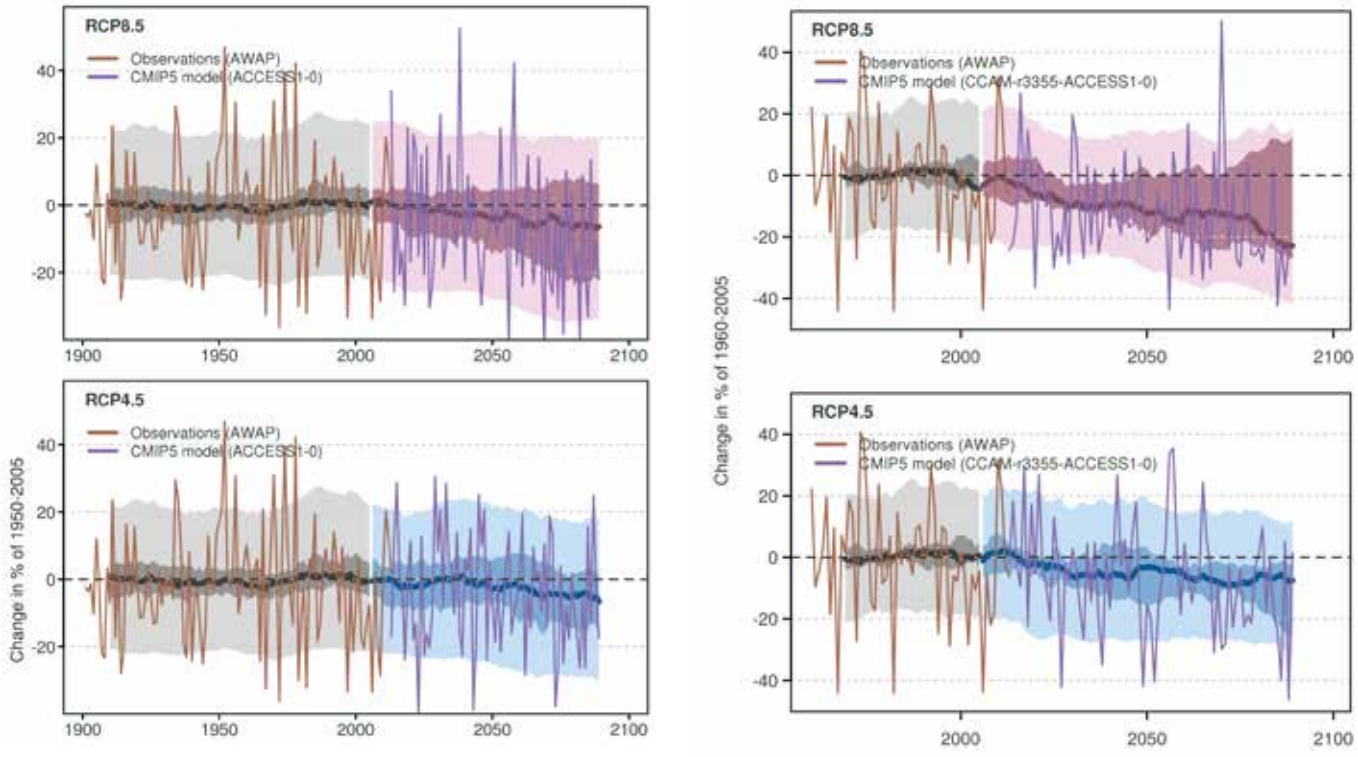

Figure 34. Projected change in Victorian annual average rainfall from CMIP5 (left) and CCAM (right) under different RCPs, showing general agreement for a decrease in rainfall but with a spread of model results and high climate variability (see box on page 40 for details of how to interpret the plots).

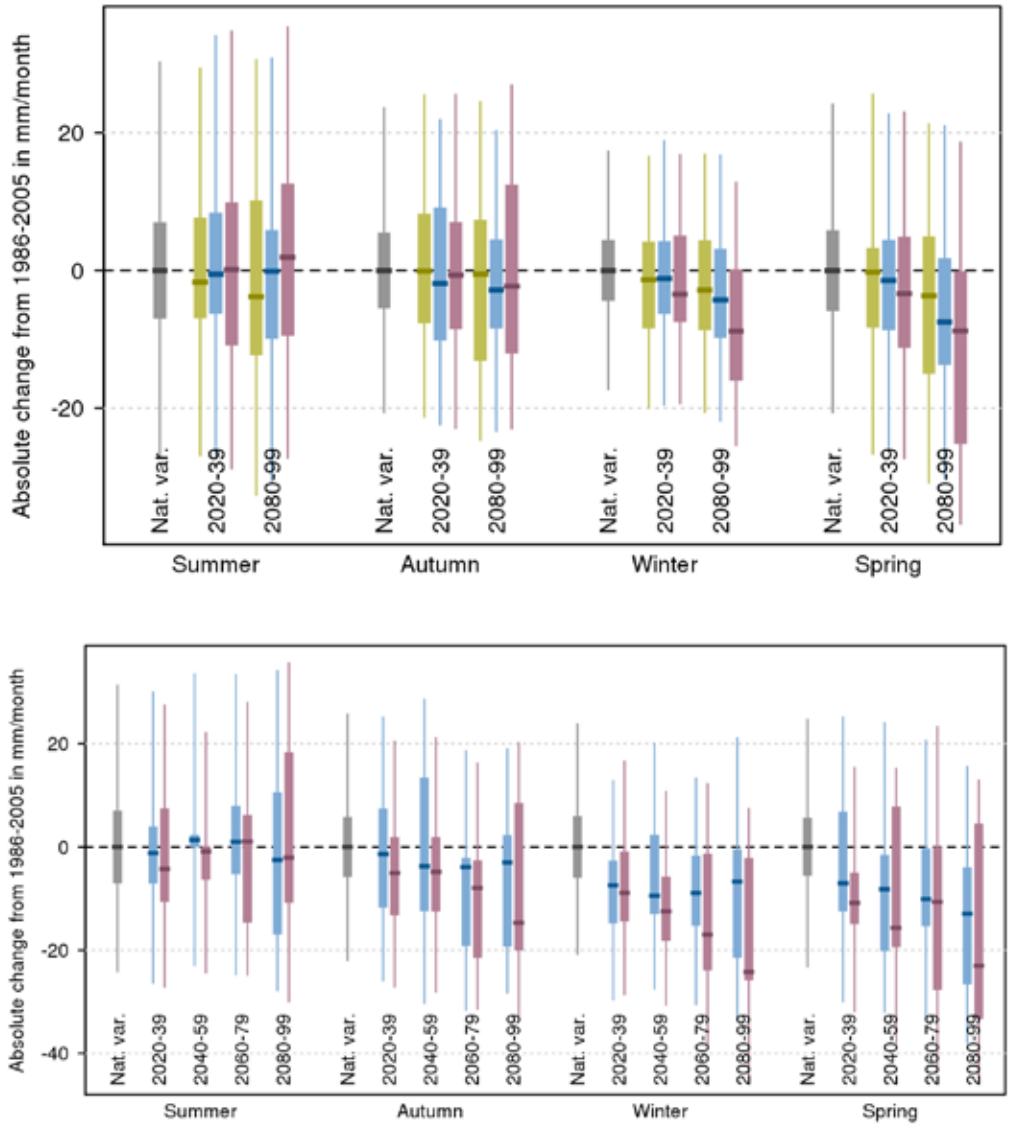

Figure 35. Bar plots of projected change in Victorian average rainfall (mm/month) in the calendar seasons for different future time windows and RCPs from: top: CMIP5 projections for two time periods and three RCPs, and bottom: VCP19 runs for four time periods and two RCPs. Green is RCP2.6, blue is RCP4.5, red is RCP8.5 and grey shows the range of change expected from natural variability alone (see box on page 40 above for details of how to interpret the plots, including bars, stems and dark lines)

Maps of change for individual model projections show the spatial distribution of projected rainfall change through time and by season. Projected change in annual rainfall in each model under the high emissions scenario RCP8.5 (Figure 36) reflects the high model agreement for rainfall decrease through most future periods, with different magnitude of decrease in different models. The plot also shows that the model with the wet projection (NorESM1-M) in fact shows little change or a projected decrease in rainfall through most of the century up until the 2090 time slice. Looking by season, Figure 37 shows the multi-model average change for the high emissions scenario, towards the end of the 21st century (20-year period centred on 2090 for all ensembles except NARCliM) to illustrate strong change signals and draw out the differences among data sets, seasons and regions. In this case, results from five sets of earlier projections data are compared with the new VCP19 runs (see Table 2 for details of the data sets). The projections from individual runs of VCP19 are shown in Figure 38.

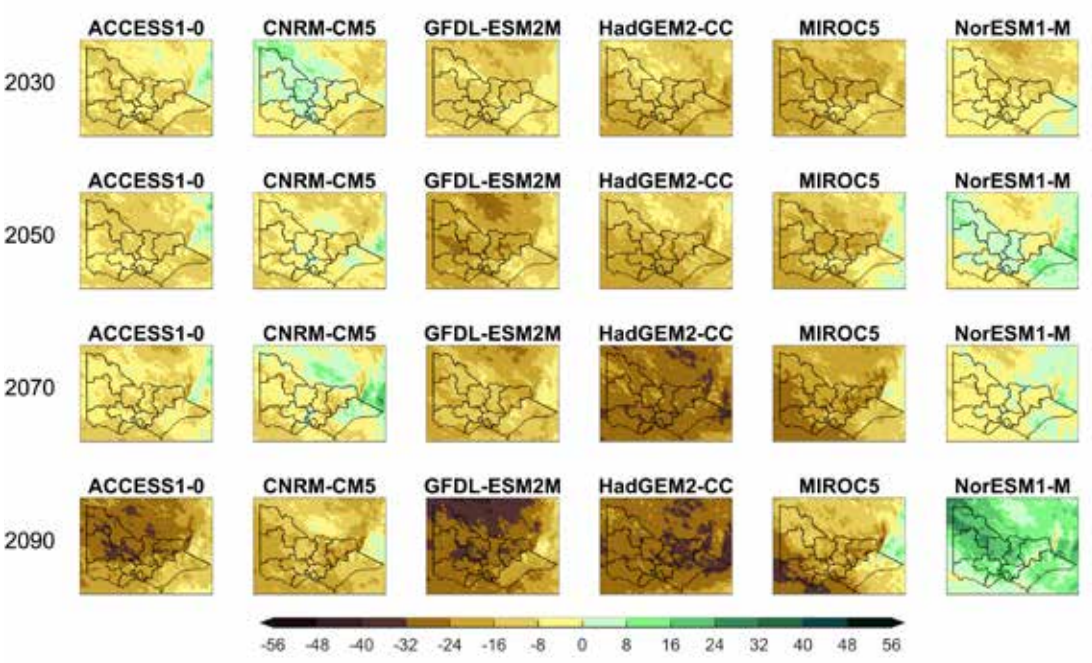

Figure 36. Projected change in annual rainfall (%) under high emissions (RCP8.5) for each of the six VCP19 CCAM simulations between 1986–2005 and four 20-year future periods centred on 2030, 2050, 2070 and 2090 (models are downscaled using CCAM and are labelled using the name of the GCM used as input).

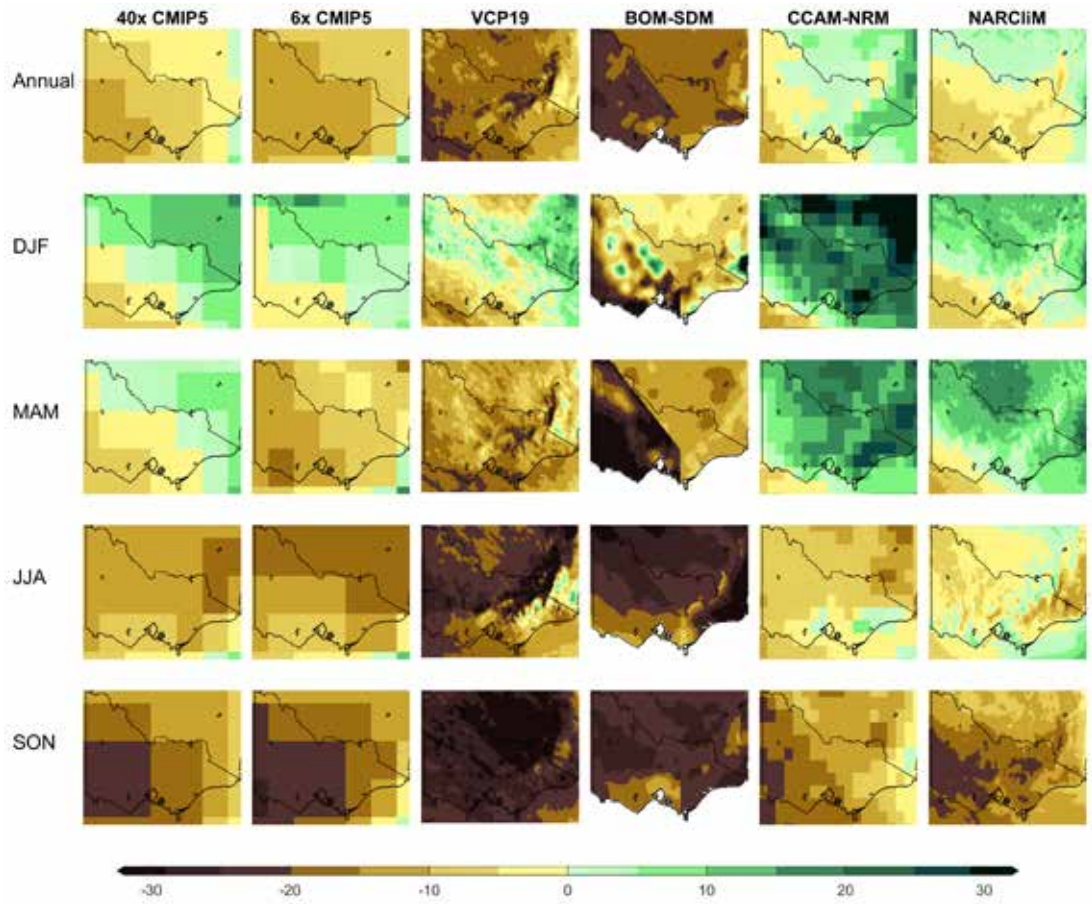

Figure 37. Model mean projected change (%) in annual average rainfall from different sets of model output: 40 CMIP5 models, the six CMIP5 models used as input to VCP19, the six new CCAM runs for VCP19, 23 runs of the Bureau of Meteorology statistical downscaling model (BOM-SDM), six 50-km CCAM runs done previously for the NRM project, and 12 runs from the NARCliM project. Change is shown for 1986–2005 to 2080–2099 under RCP8.5 except NARCliM which shows 1990–2009 to 2070–2089 under SRES A2.

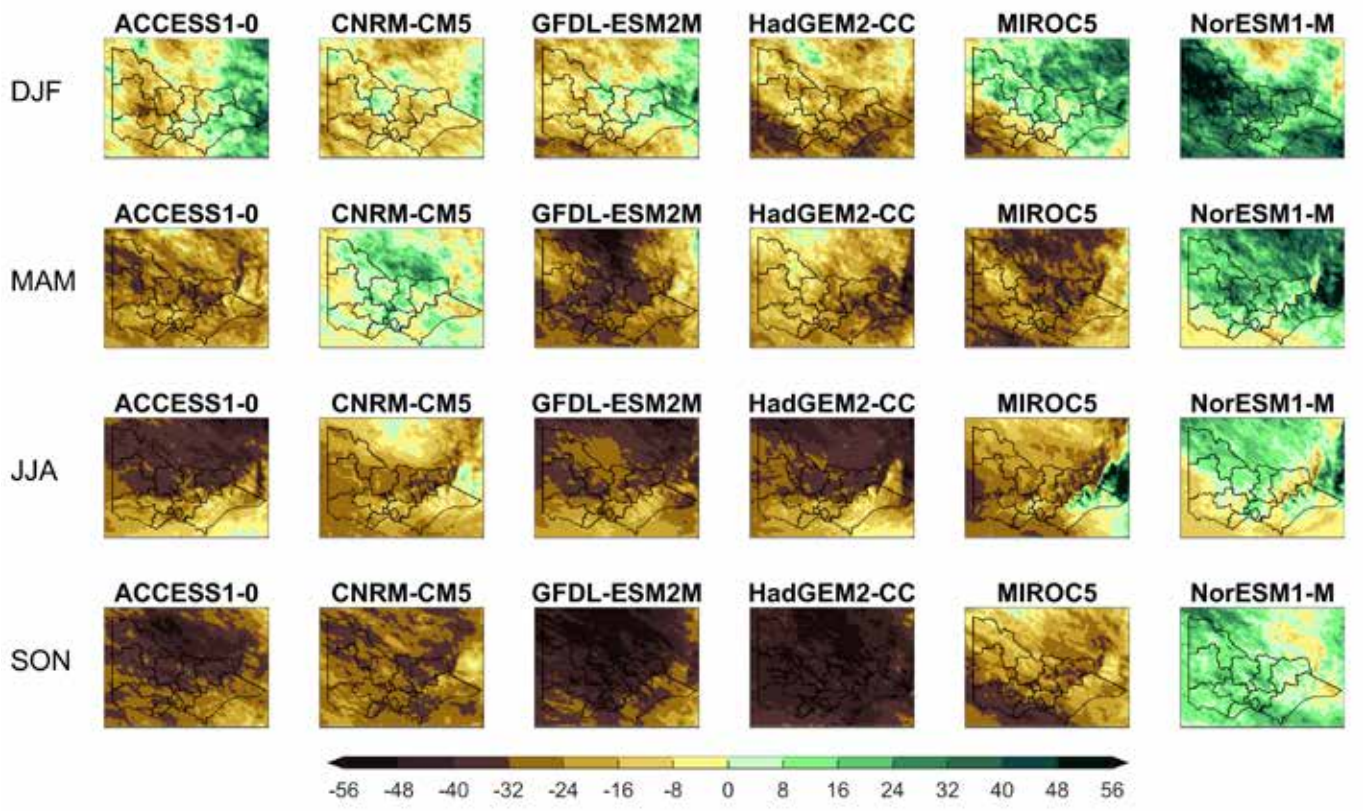

Figure 38. Projected change in rainfall (%) between 1986–2005 and 2080–2099 under RCP8.5 for each calendar season for each of the six VCP19 simulations (models are downscaled using CCAM and are labelled using the name of the GCM used as input).

At the broad scale, the mean of the VCP19 ensemble shows a decrease in annual, summer and autumn rainfall, which is more consistent with CMIP5 and the six host models than the previous dynamically downscaled projections from NRM-CCAM and NARCliM, but not as severe as BOM-SDM. The projected decrease in rainfall from new CCAM in winter and spring is greater than the host models and is comparable to BOM-SDM used for VicCI. Results from individual models show that generally four or five models agree on the sign of change in all instances, with only the simulation using the NorESM1-M model projecting an increase in rainfall in all seasons in this time-slice (noting that previous time-slices are different, see Figure 36). Two models show particularly severe rainfall reductions in spring.

At the regional scale, the VCP19 runs show plausible regional detail in the spatial pattern of change over, and adjacent to, mountains – primarily an enhanced drying on the windward slopes in autumn, winter and spring. There is also, perhaps, increased rainfall over the peaks of the Alps in summer, consistent with work in the European Alps (Giorgi et al. 2016), but this is present mainly north of the Victorian border. See also Grose et al. (2019b) for details about the enhanced drying associated with topography.

These broadscale differences and regional details can be drawn out and the ranges between models in each of the ensembles can be put in context using bar plots for key VCP19 regions for this far future and high emissions scenario. Two interesting and notable cases are shown here, see individual reports for the others. Ovens Murray on the inland slopes of the Alps (Figure 39) shows the enhanced drying in the cool seasons in the VCP19 runs compared to the host models and all of CMIP5, but also shows notable overlap in the model range. The plot shows the difference from previous dynamically downscaled ensembles (NRM-CCAM, NARCliM) is very marked. Differences from BOM-SDM are not notable except in summer.

Individual VCP19 model simulations (marked as dark dots in Figure 39 and Figure 40) show the grouping of models is not even with some strong grouping in some seasons. For example, in spring, there are five simulations that indicate marked drying, but one simulation indicates a wetter future. This is largely related to the host models, chosen to be representative of the complete set of CMIP5 models that show this range, but there is also some effect from the simulation by CCAM as well.

Enhanced drying on the western slopes of the Alps in cool seasons

By resolving the mountain ranges of Victoria, the new modelling reveals a physically plausible regional pattern of projected rainfall change, with high agreement across models for a greater projected decrease on the western windward slopes and some models indicating little change on the eastern slopes.

Possible reasons: physical response of the air flow over mountains in a warmer climate

Seasons: autumn, winter and spring

Regions: particularly Ovens Murray, but other regions too

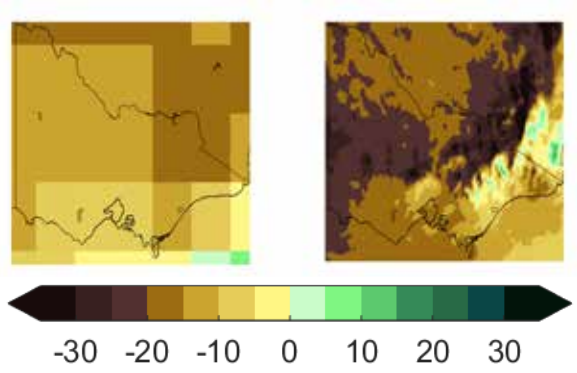

Projected change in winter rainfall – RCP8.5 by 2090, in the average of six GCM simulations and six CCAM simulations from those GCMs

Grose et al. (2019b) propose that the change in convective rainfall may determine the sign of change in this season inland of the mountains. Such a change will be accounted for in GCMs and dynamical downscaling but not in analogue-based statistical downscaling (e.g. BOM-SDM), which may explain this difference in results. There are notable differences between VCP19 runs and NARCliM, which is likely to be partly due to model selection (the projects used completely different models as input) and also the configurations of the dynamical downscaling models. The ensemble of configurations chosen for the modelling system used in NARCliM are specifically chosen to encompass a wide range of possible rainfall results (e.g. Di Virgilio et al. 2019). Figure 39 shows that the ranges of CMIP5 and the six host models (6xGCMs) are similar, supporting the selection of models as broadly representative in temperature and rainfall change. For the Greater Melbourne region (Figure 40), the results are similar but the differences among ensembles are less pronounced.

An alternative to using any one ensemble in isolation, or considering them all separately, is to produce a combined ensemble distribution of all inputs. This is shown as a black bar in Figure 39 and Figure 40, and uses randomly drawn data from each ensemble, with equal weighting given to each set of inputs, to produce a new statistical sample. See Ekström et al. (2007) for more detail of the methods, and Grose et al. (2015b) for another example of its use. Note that the bar does not cover the entire range of all the bars from input data sets, as the very ends are not shown (the 10th to 90th percentile range is shown). Without a compelling, documented rationale why one set of inputs should be rejected, then the entire range of this black bar should be considered possible.

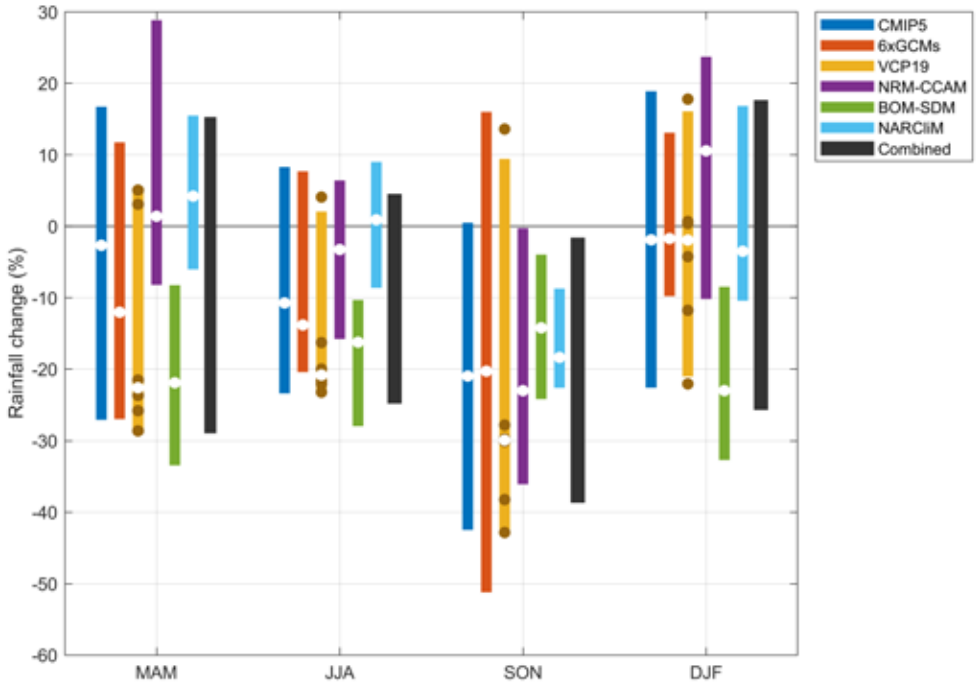

Figure 39. Projected rainfall change for the Ovens Murray (OVM) region, showing the different ranges of projected change for each season from each ensemble of models and a distribution that combines them all (bars show the 10th to 90th percentile range of results, white circle shows the median).

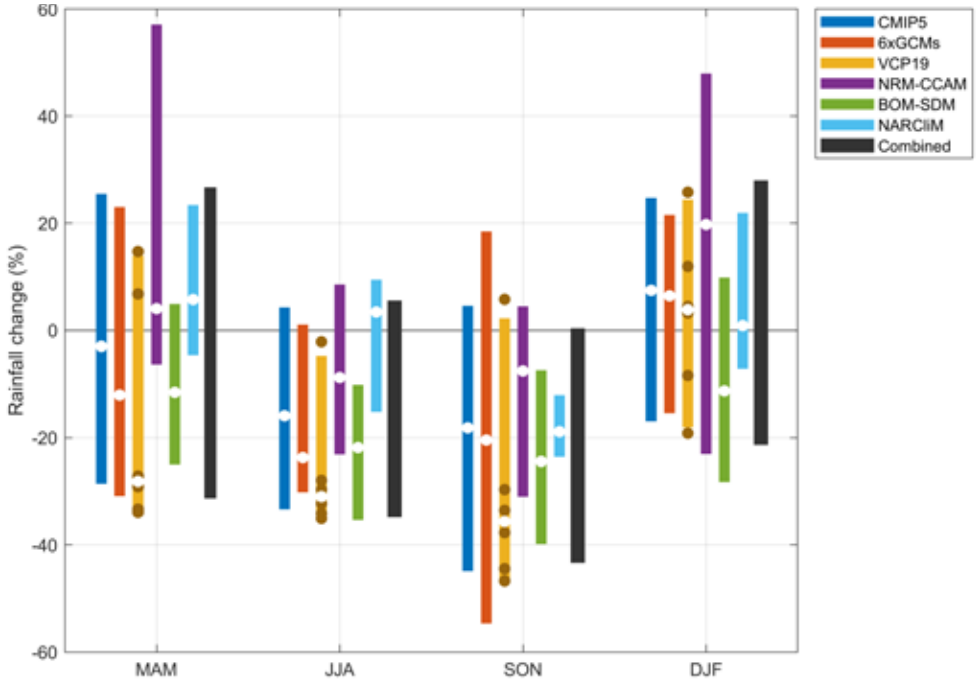

Figure 40. Projected rainfall change for the Greater Melbourne (MET) region, showing the different ranges of projected change for each season from each ensemble of models and a distribution that combines them all (bars show the 10th to 90th percentile range of results, white circle shows the median).

All downscaling approaches are aimed at producing plausible regional projections of a change in the climate. A high level of agreement among different ensembles provides strong evidence that any regional-scale changes are plausible. However, the new VCP19 runs present a different view of future rainfall than previous dynamical downscaling from an earlier (and lower resolution) version of CCAM (the NRM-CCAM runs) and the NARCliM runs, particularly for summer and autumn. The VCP19 runs do agree with previous statistical downscaling (BOM-SDM) in some important aspects while differing in others (e.g. in the most extreme dry projection and the summer projection). This raises the question of why the different ensembles give different results, and if any ensemble should be weighted lower than any other for being less physically plausible or otherwise lower in confidence than the others.

There are two main explanations for a difference between the downscaling ensembles: the choice of host models from which to downscale, and details of the dynamical interactions within the model. The new CCAM results are different from previous CCAM results for a combination of both reasons. The NRM-CCAM used three host models in common with the VCP19 runs but three that were different. This explains some of the difference. The selection of host models used for VCP19 was drawn wholly from the representative set selected by *Climate Change in Australia*. In contrast, NRM-CCAM used only three of these models as hosts. As described in section 2.2, the set of six host models used for the VCP19 runs is broadly representative of the full CMIP5 archive, with some gaps (compare panels in Figure 37, and bars in Figure 39 and Figure 40).

In terms of model design, the version of CCAM used for the VCP19 runs is higher resolution (5 km compared to 50 km for NRM-CCAM) and has had ongoing model development since the version used for the NRM-CCAM simulations. Accordingly, the new version produces different results. The MSLP and circulation response in the CCAM simulations is different than the GCM hosts (see section 5.4), possibly due to a different response to the surface warming pattern, and this may play a role in creating a different rainfall projection. However, we are not able to determine whether the CCAM response is more or less plausible than the GCMs.

The influence of the downscaling model (rather than host model choice) is shown in Figure 41 where autumn rainfall is projected by the ensemble of the three host models that were common to both the NRM-CCAM and VCP19 runs. This shows that the average of the three GCMs (panel a) projects a decrease in rainfall, whereas the average of the three NRM-CCAM runs (panel b) projects a rainfall increase. The average of the three VCP19 simulations (panel c) projects mainly a decrease in rainfall similar to the host models but with a regional pattern mainly related to topography (a physically plausible pattern, see Grose et al. (2019b)). The average of three BOM-SDM simulations (panel d) projects mainly a decrease in rainfall but with greater magnitude and with some artificial hard boundaries related to the model set up (e.g. the boundary bisecting the Gippsland region).

The added value from the downscaling in the spatial pattern of projected change over mountain regions in response to the topography is presented with *medium to high confidence*, as there is a physical explanation for the difference from GCMs laid out in a peer-reviewed paper (Grose et al. 2019b) and agreement with other modelling systems and recent observed changes. However, the confidence in the broader rainfall projection being reliable is lower, since model agreement is lower.

It is impossible to comprehensively demonstrate which projection is more reliable, since we cannot check against the actual rainfall change to 2090 under that exact emissions scenario. However, the improved representativeness of the host model selection and the similarity of the regional pattern of change with the host models, coupled with physically plausible enhanced regional detail are two lines of evidence supporting the VCP19 projections being physically plausible. In contrast, a case would have to be made that the increases simulated by NRM-CCAM or the greater decreases produced by the BOM-SDM are more physically plausible than other sources of information for them to be used in isolation. To date, such a case has not been made. Therefore, CCAM projections should not be used in isolation and instead the full range of projected change in rainfall (black bars in Figure 39 and Figure 40) should be considered plausible. Also, the median of the six CCAM runs should not be considered as a single 'best estimate' of change, particularly for the dry projection in spring. Instead, a scenario-based approach should be taken, sampling from the full range of possibilities, and including cases from CCAM.

Figure 42 further tests the assertion that the projected changes in rainfall in the VCP19 results are consistent with the broader projection of the CMIP5 GCMs, but with added regional detail over mountains and near coasts. Each panel shows the ensemble average for the CMIP5 GCMs over the southeastern corner of Australia, with the VCP19 ensemble averages superimposed over just a rectangle encompassing Victoria. There are relatively few discontinuities between the spatial patterns of change in the two domains, but with higher resolution patterns within the Victorian domain.

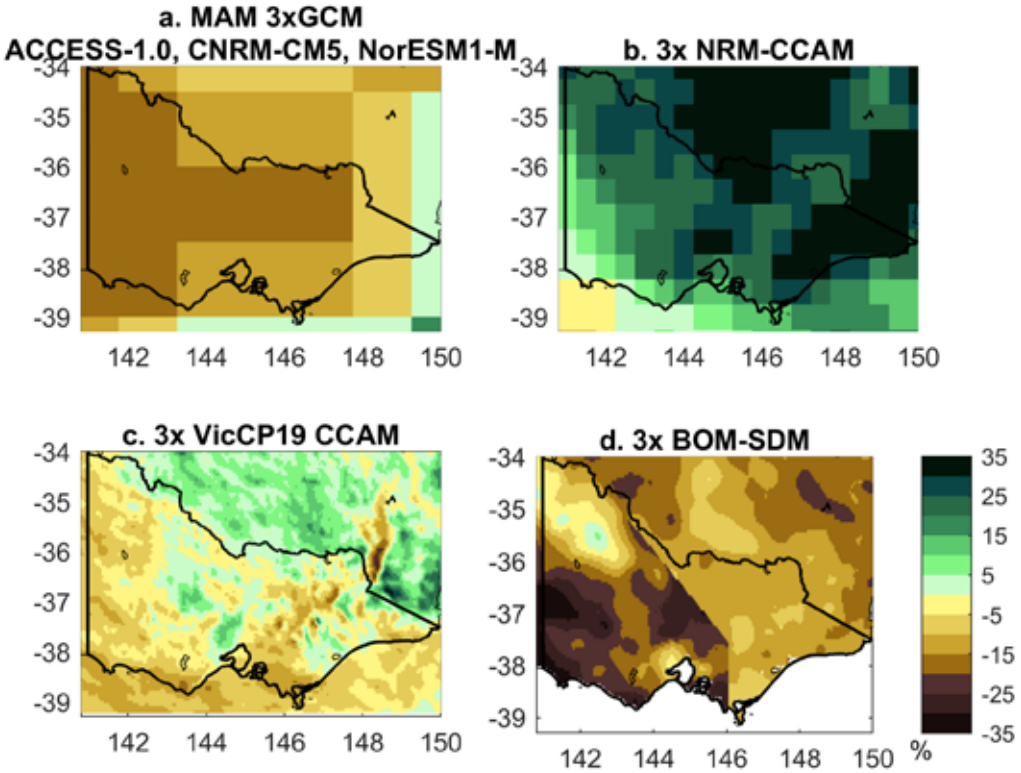

Figure 41. Comparison of the model average projected change in average rainfall between 1986–2005 and 2080–2099 in three GCMs and three downscaling ensembles that use those GCMs as input.

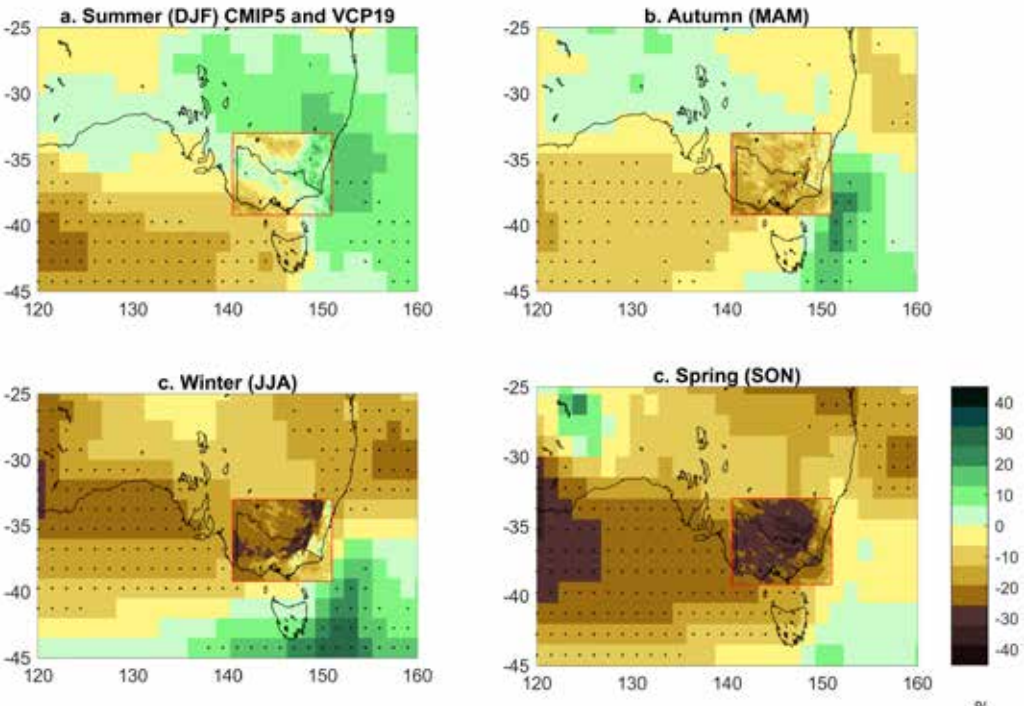

Figure 42. Projected change in rainfall between 1986–2005 and 2080–2099 under RCP8.5 in 45 CMIP5 models over Australia, overlaid with the average of six VCP19 simulations over the Victorian region in four calendar seasons as marked. Stippling is only shown for GCMs and indicates where 80% or more of models agree on the sign of change (more than 35 of the 45 models).

5.3.4 Snow

No new analysis of projected changes to snow cover or snow depth is presented here, but a preliminary analysis of the new simulations show they confirm previous findings regarding projected changes to snowfalls and snow cover. Snow depth and the spatial extent of snow cover have been decreasing since the 1950s at many locations in Victoria, with the largest declines during spring. Snow depths are related to temperatures, and the decline is linked to the warming experienced (Davis 2013). In future, snow depths and snow extent are projected to continue decreasing, due to reductions in snowfall and increases in snow melt. The magnitude of the reduction depends on the emissions scenario, where considerable reductions to very low snow cover is projected under a high scenario, but significant reductions even under a moderate scenario. Ski resorts can supplement a lack of natural snow with snow making up to a point, but eventually this can become unviable. Various natural ecosystems and alpine species of animals and plants are vulnerable to a warmer climate and cannot retreat to higher ground since they are already in alpine regions. For more detailed analysis, see the national climate projections and other previous studies (Nicholls 2005; Hennessy et al. 2008; Bhend et al. 2012; CSIRO and Bureau of Meteorology 2015; Harris et al. 2016).

5.3.5 Rainfall extremes

A warmer atmosphere can hold more moisture, so with all else being equal, heavy rainfall at the scale of minutes to a day is expected to increase in most places and seasons as a general response. This has been observed at the continental scale in hourly data, at close to or above the expected rate of about 6.5% per degree of global warming (%°C GW^{-1}, (Guerreiro et al. 2018a)). We expect this to be important for hourly to daily rainfall extremes in Victoria both in the current climate and in future. This process can be offset or enhanced by changes to the intensity, frequency or other characteristics of the weather systems that bring heavy rainfall. For example, the future of the strongest cold fronts, thunderstorms, east coast lows or extra-tropical cyclones is important to understanding future extreme rainfall.

In places where average rainfall is projected to decrease slightly, the rainfall from wet days, heavy rainfalls and extreme daily rainfall is still projected to increase under a high emissions scenario. This was the main finding from the most recent GCM-based projections for southern Australia generally, including Victoria (CSIRO and Bureau of Meteorology 2015). The increase was largest for the rarest extremes. That is, the 1-in-20-year daily rainfall (ARI20) was projected to increase by more than the annual wettest day (calculated over a 20-year period). For example, in the Southern Slopes Victoria West region under a moderate scenario (RCP4.5) by the end of the century, the range of projected change in annual average rainfall was mainly negative (-15 to +3%, median -7%), but the range of ARI20 was mainly positive (-7 to +39%, median of +15%). In comparison, changes to the rainfall on heavy rain days (amount of rainfall on days above the 99th percentile) was projected to increase but with a large range of possibilities (-10 to +76%, median of 18%). Under the lowest scenario (RCP2.6) changes were much less pronounced (and indeed, mean annual rainfall was projected to change less, with a range of -13 to 3%, median of -3%). (For more detail, see CSIRO and Bureau of Meteorology (2015) and the *Climate Change in Australia* website[4]).

The new VCP19 downscaling results support the previous projections for a likely increase in daily rainfall extremes under a high or medium emissions scenario, despite decreases in average rainfall (Figure 43) and with a range of changes possible. This suggests that the higher resolution of atmospheric processes in VCP19 runs (5 km over Victoria compared to 60 km or more in GCMs) does not alter the projection significantly. There is the possible exception in the central regions of Loddon Campaspe (LOC), Goulburn (GOU) and Ovens Murray (OVM) under RCP8.5, where VCP19 runs projected increase in the magnitude of daily rainfall extremes is not as large. This suggests the stronger drying projected by VCP19 runs and the simulated changes to the relevant weather systems result in a lower projection, creating a plausible lower scenario of change.

Given the physical evidence, agreement among models and previous research, an increase in intense rainfall at the hourly to daily scale is projected with *high confidence*, but the magnitude of the change is less certain. It is possible that further new insights could be found using extremely high-resolution modelling (e.g. 1.5 km) that is capable of simulating convection at finer spatial scales.

4 www.climatechangeinaustralia.gov.au

Compound extremes

Extreme events in one climate variable (e.g. hot days, very wet days) can have important impacts, but events with the greatest impact are often those with extremes of multiple variables and those that occur simultaneously or in succession, including:

- extreme storm surge and extreme rainfall and winds occurring as part of an intense low-pressure system
- a prolonged heatwave and/or extreme heat days during a drought
- drought and heat leading to higher fire danger
- a series of extremes with cascading impacts, such as Tasmania experienced in 2015–16 (hot, dry spring and summer, fires, a marine heatwave, floods, then a very wet period).

Climate change will affect the incidence of extremes in different climate variables, but also in the chances of compound events (e.g. sea-level rise and increasing intensity of short-duration rainfall may both increase flood risk in vulnerable estuaries). Modelling compound events is a challenging task for several reasons including the lack of high-quality data sets and is an ongoing area of research.

This projected increase in daily extremes is likely to result in unprecedented events of heavy rainfall and therefore flash flooding. The current record highest daily rainfalls at weather stations anywhere in Victoria are 375 mm at Tanybryn in the Otway Ranges in March 1983, followed by 319 mm at Mount Wellington in June 2007 and 300 mm at Rotamah Island in November 1988. To give a more commensurate comparison to VCP19 runs produced on a grid, these three records in gridded AWAP data do not exceed 209 mm. Figure 44 shows an example very wet day as simulated by the VCP19 modelling under high emissions towards the end of the century. This example shows the possibility that many regions could receive more than 150 mm in 24 hours. It also shows a plausible record daily rainfall in some areas of more than 300 mm. Note that this is not the highest daily event in the projection data but it is representative of a high event.

The projections paint a picture of a drying climate but an increase in daily rainfall extremes. There is also a projected increase in sub-daily extremes, in line with recent trends (Guerreiro et al. 2018b). This has the effect of changing the shape of rainfall intensity, frequency and duration (IFD) curves used in applications such as infrastructure engineering. An increase in the intensity of short duration rainfall (minutes to a day or so) drives an increase in one end of the curve, but a decrease in longer duration rainfall (weeks to months) at the other end of the curve. The response may also be different for the curves for different return periods. Given that projected changes are different for different regions and there is a range of change from different models, the strength and significance of these changes needs to be specifically assessed for any particular application.

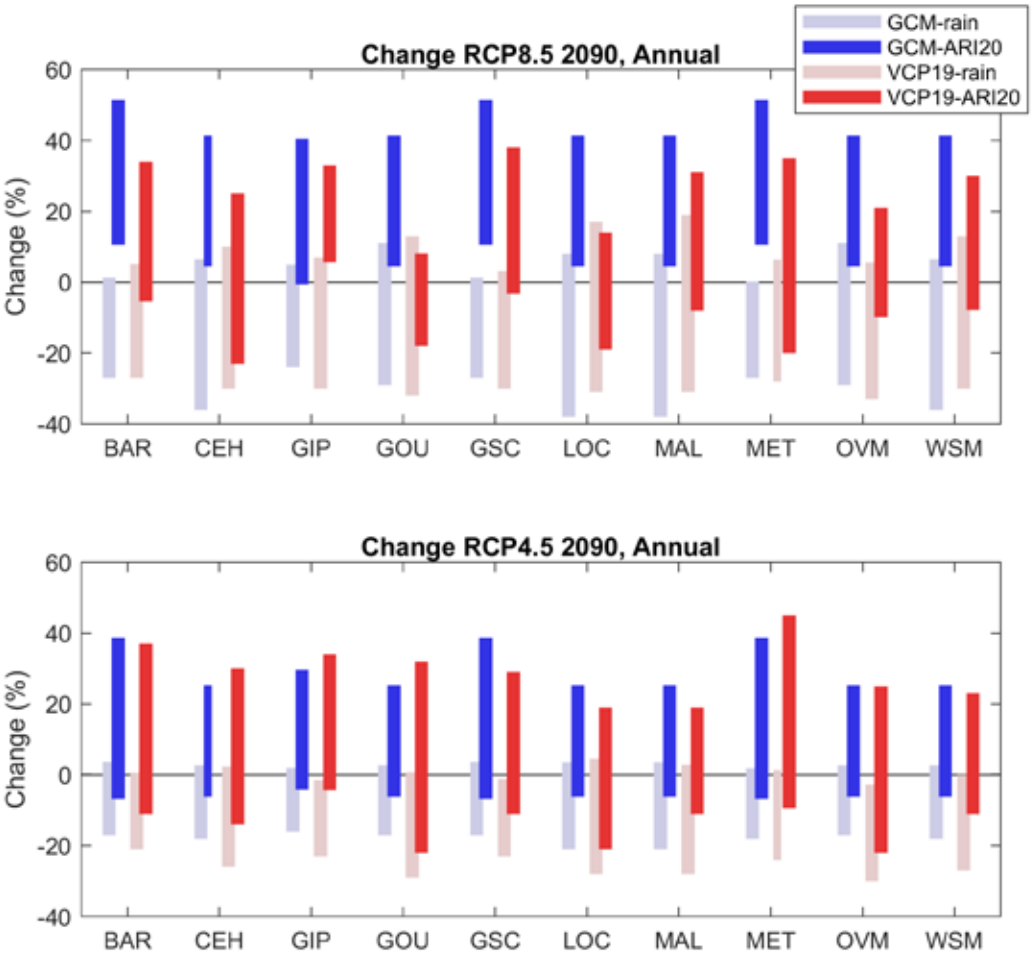

Figure 43. Proportional projected change to average and extreme (ARI20) rainfall between 1986–2005 and 2080–2099 in GCMs and VCP19 runs annually under RCP8.5 and RCP4.5 for the 10 VCP19 regions, showing generally a decrease in rainfall and an increase in extreme rainfall. The 10 high-resolution VCP19 regions are shown using their codes (see Table 4 for full names)

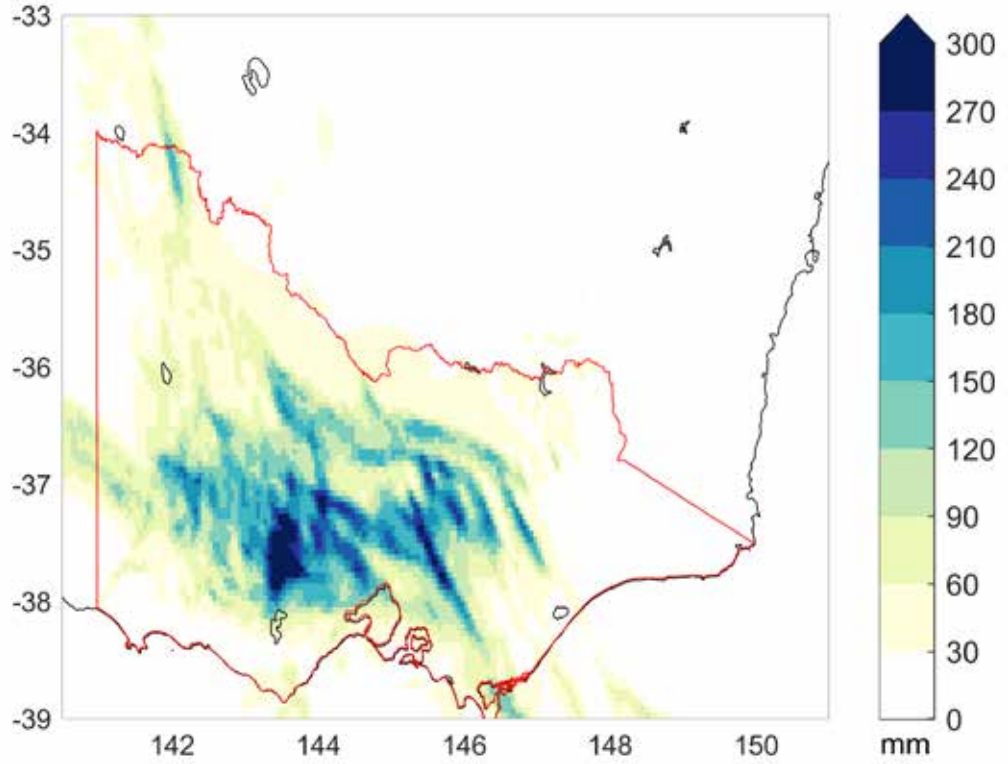

Figure 44. Daily rainfall for an example heavy rainfall day in the far future under the high scenario (2090s under RCP8.5 in the NorESM1-M model downscaled using CCAM). Note this is not the most extreme rainfall event in the simulations, just an example of a very wet event. Also note that extremes are projected to occur in all regions and the locations of the extremes this is just one example event.

5.4 Mean sea-level pressure

As the climate warms, mean sea-level pressure (MSLP) is projected to decrease near the south and north poles and increase in the mid-latitude regions such as Victoria. This projected change is consistent with the changes in the broad hemispheric circulation patterns including changes to the Hadley Cell, storm tracks and SAM (Collins et al. 2013). The projected change in MSLP is not uniform around the hemisphere (see Figure 7.2.11 in the national climate projections (CSIRO and Bureau of Meteorology 2015)), and the spatial pattern of change affects the regional climate change experienced at any location. In winter under a high emissions scenario by the end of the century, GCMs project a significant increase in MSLP either side of Australia and a region of weaker MSLP increase over the south of the continent. In summer, MSLP is projected to increase to the southwest of the continent with little change or even decrease over the continent itself. This pattern is broadly represented in the six GCMs used in these projections (Figure 45). The projected change in MSLP in the average of the six 50 km CCAM simulations using these GCMs as input shows broadly the same pattern as the GCMs, but with a few notable differences. In summer and autumn, the pressure response over land is enhanced, where the MSLP is projected to decrease to a greater degree than the GCMs. This is possibly due to a different response of the CCAM model to the land-ocean contrast in temperature than the GCMs, as found previously (Grose et al. 2015b). In winter, the centre of the peak in increase in MSLP is further east than in the

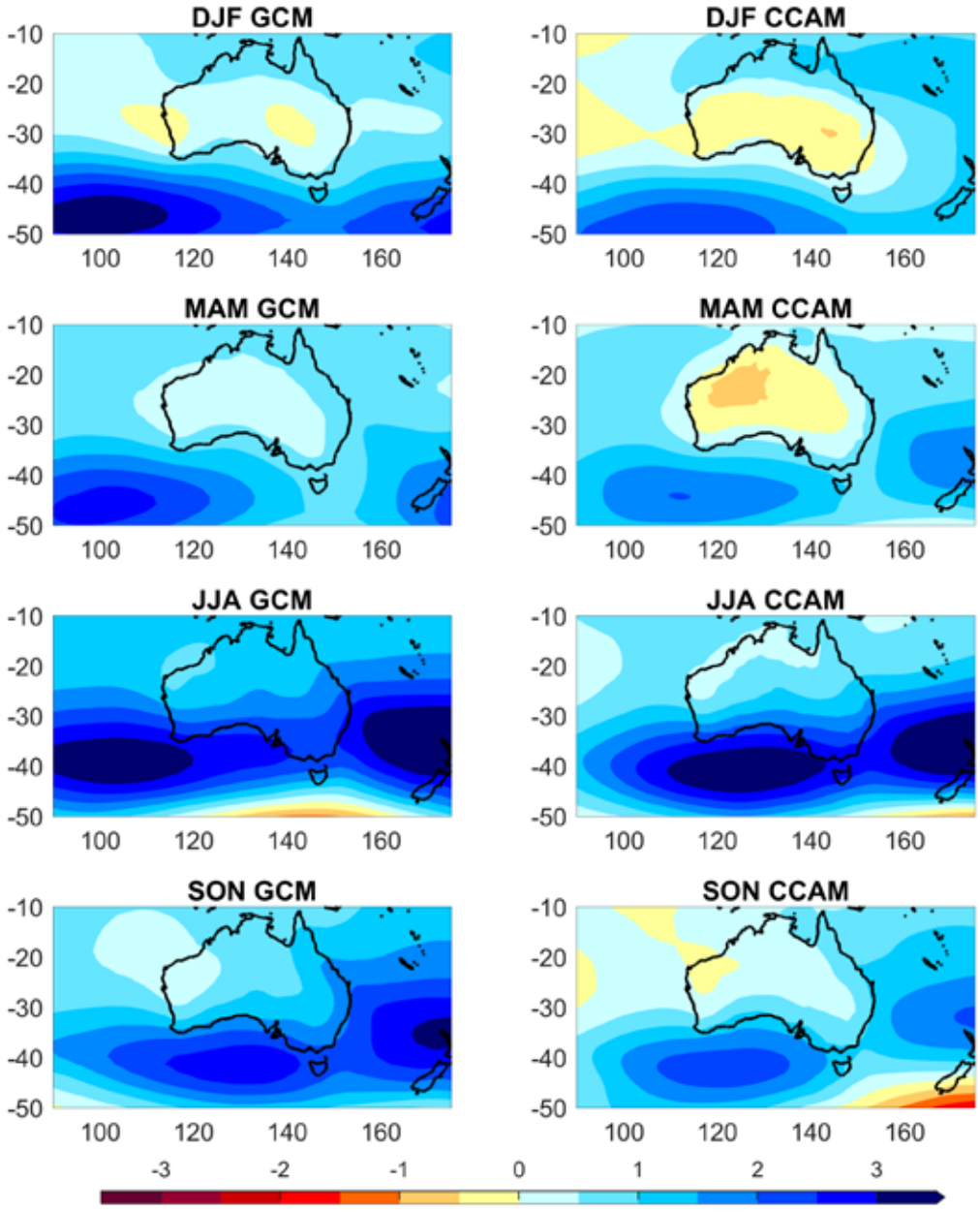

Figure 45. Model-average projected change in mean sea-level pressure (MSLP) in hPa between 1986–2005 and 2080–2099 under a high emissions scenario RCP8.5; left: average of the six GCMs used as input to VCP19; right: six ~50 km CCAM simulations used in VCP19. By calendar season.

GCM hosts, bringing it close to Victoria. These differences are expected to create a different circulation anomaly over the region of southern Australia in CCAM than in the GCMs, and possibly affect the rainfall projection. However, the broadscale rainfall projection is similar between CCAM and the GCMs (see previous section), so this effect may not be significant. It is also not clear whether the difference between the CCAM-simulated change in MSLP compared to the host GCMs less or more physically plausible or realistic than the GCMs, so it is not possible to determine whether it should be seen with lower or higher confidence than the CMIP projection.

5.5 Winds and storms

5.5.1 Mean winds

Wind patterns are determined by the location and seasonal movement of broad atmospheric circulations and weather systems. During the cool seasons, the subtropical ridge is north of Victoria and experiences dominant westerly circulation, but with periods counter to this mean flow. In summer there is a mixture of circulation patterns over Victoria.

Over the 21st century, westerly 10 m wind speeds in winter are projected to decrease over southern Australia due to weakening circulation, affecting 10 m wind speeds in southern Western Australia. However, this effect is not clearly expressed over Victoria in climate models. The projected changes in 10 m wind speed in all seasons are generally small even under the highest emissions scenarios (<10% magnitude), with low agreement on the strength and direction of change (CSIRO and Bureau of Meteorology 2015).

The new VCP19 simulations are consistent with previous climate model simulations, with projected changes in the 10 m wind speed of less than 10% (mostly less than 5%) even under RCP8.5 by the end of the century, and low agreement on the magnitude or even sign of change in all VCP19 regions. This suggests that average 10 m wind speed over Victoria is unlikely to change significantly over the century.

5.5.2 Extreme winds

High wind speeds are determined by the same atmospheric circulation and weather systems as mean winds but are modified by surface features like terrain and vegetation. GCMs do not resolve the surface features such as hills and valleys and will poorly resolve the winds associated with the systems that bring strong winds such as thunderstorm downbursts. The 5 km resolution of the VCP19 modelling resolves these features to a much greater extent, so there may be events and highly localised trends in 10 m wind speed that are notable (this requires further specialist analysis and could be the subject of further research).

The national climate projections (CSIRO and Bureau of Meteorology 2015) reported that notable changes in extreme 10 m wind speed in annual maximum and 20-year return period (ARI20) 10 m wind speeds are possible in Victoria, but the magnitude and even the sign of change was uncertain. The model median was for a slight decrease in 20-year return period 10 m wind speed for southern Victoria and the Murray Basin.

The new downscaled results also present a range of changes in extreme 10 m wind speed, but do not show high agreement on magnitude or even sign of change in extreme winds for each VCP19 region (Figure 46).

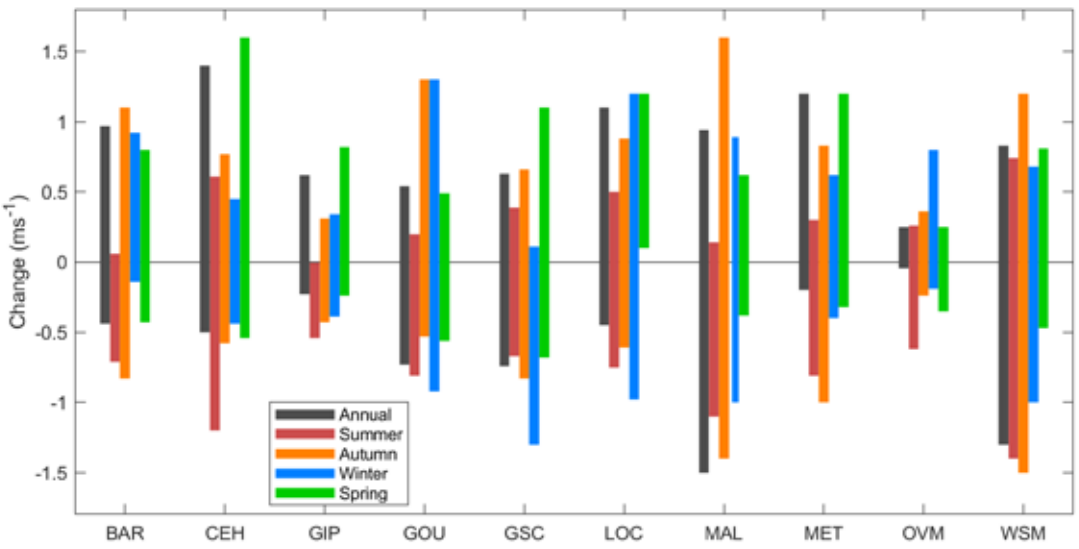

Figure 46. Projected change in 20-year return period (ARI20) 10 m wind speeds between 1986–2005 and 2080–2099 under RCP8.5 for each VCP19 region. The 10 high-resolution VCP19 regions are shown using their codes (see Table 4 for full names).

Changes in 20-year return period 10 m wind speed are shown in absolute magnitude (ms^{-1}), and the magnitude of change is partly related to differences in the current value (larger changes on larger current values). There are some differences between regions that make sense given current knowledge of climate change. For example, the only region with high agreement on decreased 20-year return period 10 m wind speed in winter is the Great South Coast, which is consistent with reduced westerly circulation known to affect southwest Western Australia and other western coasts.

5.5.3 Storms and lightning

Interpreting changes in storms and lightning is a challenge for both GCMs and RCMs. This is because the important processes are also not well resolve by the RCM simulation. Examining the Convective Available Potential Energy (CAPE) can provide an indication of favourable conditions for forming thunderstorms. Projected changes in CAPE can be sensitive to the convective parameterisation used by the atmospheric model, which is an active research area of atmospheric and climate modelling. However, in broad terms the CCAM downscaled results suggest an increase in the favourable conditions for thunderstorm formation under global warming. Further research and additional downscaling experiments by different models will be required to better understand how thunderstorms will change in the future.

5.6 Relative humidity

Humidity is a measure of water vapour content in the atmosphere. Humidity near the Earth's surface is important for many processes, including transpiration by plants, fire behaviour and human comfort. There are several measures of humidity, such as specific, absolute and relative humidity. A related measure is dewpoint – the temperature at which water vapour condenses. Humidity is not routinely measured directly, but rather computed from observations of other variables, notably dewpoint. Lucas (2010) reported that there was an increasing trend in Australian averaged dewpoint values between 1957 and 2003. Over that period, dewpoint temperature increased at a rate of approximately 0.1°C per decade.

Projected changes in relative humidity (the amount of water vapour present in the air as a proportion, expressed in percent, of the maximum possible) are relatively small (Figure 47). Even under high emissions towards the end of the century, relative humidity is expected to show a median change of only -6.1% (with a range of -8.3 to +0.7%). While there are regional and seasonal differences, the projected changes are consistently relatively small and mostly show declines.

However, the projections for spring under high emissions around 2090 (Figure 48) show the strongest declines, with a range from -1.3 to -13.6%. These changes are broadly consistent with those projected using the CMIP5 GCMs (CSIRO and Bureau of Meteorology 2015).

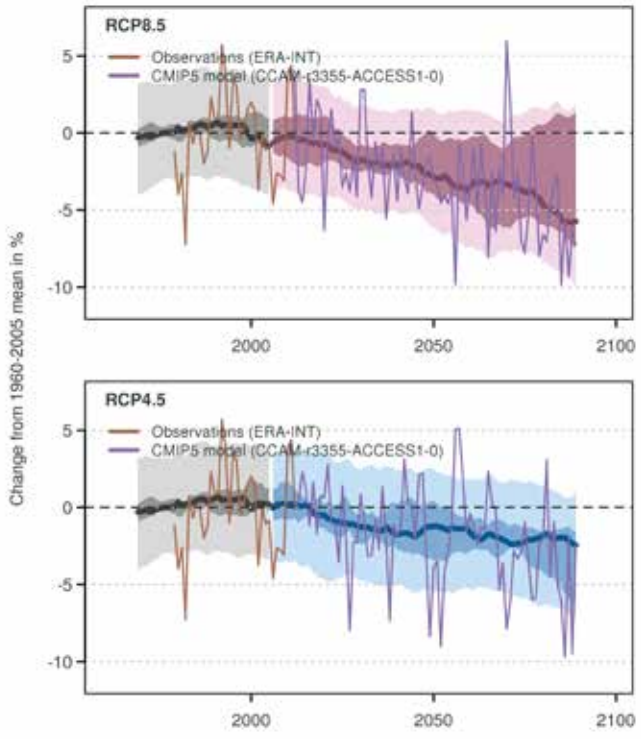

Figure 47. Time-series of relative humidity anomaly (relative to the 1960–2005 mean) from 1960 to 2090 for all of Victoria. Brown line: historic annual averages from ERA-INT; purple line: sample model results from CCAM-ACCESS1-0. For additional details on interpreting this plot, see the box on page 40.

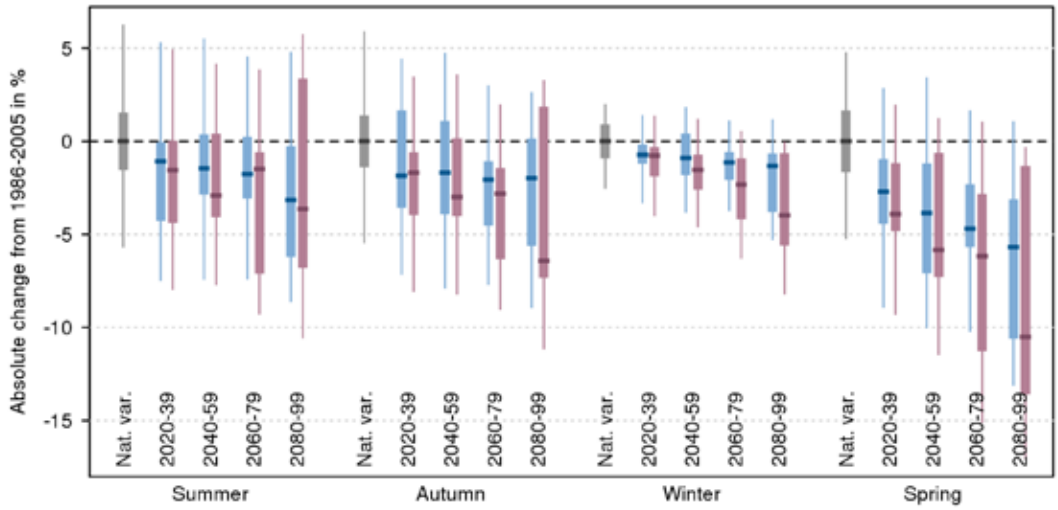

Figure 48. Bar plots of projected change in Victorian average relative humidity (%) in the calendar seasons for different future time windows and RCPs (see box on page 40 for details of how to interpret the plots)

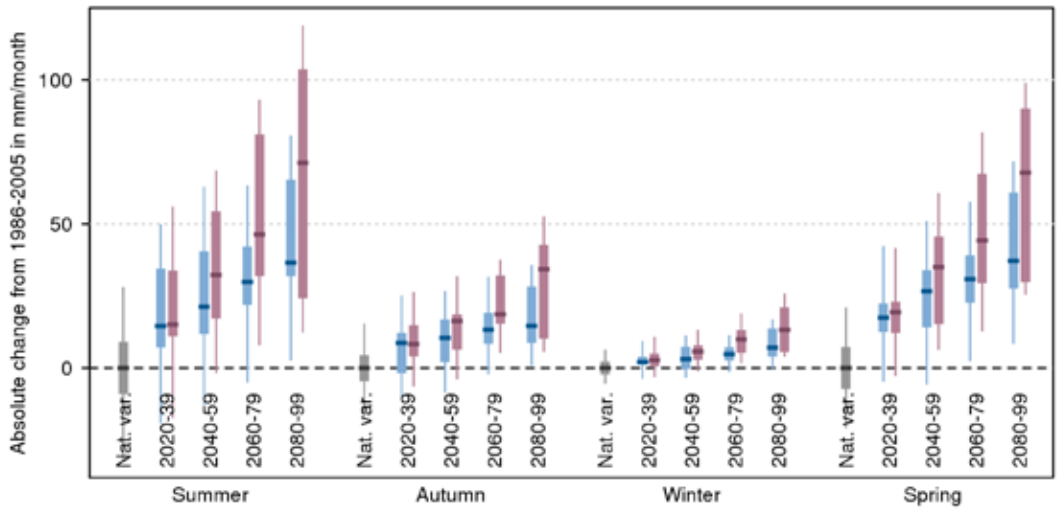

Figure 49. Bar plots of projected change in Victorian average pan evaporation in the calendar seasons for different future time windows and RCPs (see box on page 40 for details of how to interpret the plots).

5.7 Evaporation

Like relative humidity, evaporation is important for many applications, including agriculture (transpiration), water management and human health. Here we report on pan evaporation (the evaporative loss from a small body of water). Pan evaporation is modelled directly by CCAM whereas with GCM data, it must be estimated from other variables (see *point potential evapotranspiration* data on the CCIA website).

Pan evaporation is projected to increase overall for Victoria, with the greatest increases in spring and summer (Figure 49). The VCP19 runs show the greatest increases in summer under high emissions towards the end of the century.

5.8 Fire weather

As discussed in the *Climate Change in Australia* technical report, the occurrence of fire depends on the availability of fuel, the dryness of the fuel, a form of human or natural ignition, as well as suitable weather conditions. In this section, we estimate changes in the number of fire days using the Forest Fire Danger Index (FFDI) (McArthur 1967). FFDI attempts to account for fire weather (e.g. hot, dry and windy conditions) as well as fuel dryness, as a function of temperature, humidity, wind speed and drought factor. In turn the drought factor is dependent on changing rainfall, leading to changes in soil moisture. FFDI does not account for changes in fuel load, which can also depend on changing rainfall with higher rainfall leading to increased fuel load.

Fire days are defined in this report as days when the FFDI exceeds the 95th percentile of the FFDI for 1986–2005 (i.e. the worst 365 days of FFDI over the 20-year reference period). This approach to defining fire days is based on the analysis used for the National Environmental Science Program (NESP) Earth Systems and Climate Change Hub report, Climate Change and Bushfires in Australia (in preparation). Note that the assessment of fire danger in this section is not intended to have a direct correspondence to the fire danger ratings use by the Victorian Government. Rather, this section simply attempts to provide an indication of how the projected changes in climate can influence changes in fire weather. Further work with the Victorian Government will be required to develop a formal assessment of changes in fire danger ratings, considering changes in fire intensity as well as projected changes in the number of fire days.

There have been trends towards higher FFDI yearly-average values in recent decades for southeast and southwest Australia, more incidence of extreme FFDI conditions and a longer fire season including an earlier start in spring (Dowdy 2018). The observed trend in FFDI is also expected to continue into the future under global warming. Figure 50 shows the projected change in fire days between 1986–2005 and 2080–2099 under RCP8.5 for the different CCAM downscaled GCMs, using a definition based on the 95th percentile of FFDI described above. Figure 50 shows that five of the six downscaled simulations by CCAM indicate some increase in the number of fire days, except for the CCAM projection after downscaling NorESM1-M, which indicates a decrease in the number of fire days of up to 10 days per year. Note that NorESM1-M is also the only CCAM-downscaled GCM that projected an increase in average rainfall, which has an influence on the changing fire danger under global warming scenarios. The remaining five of the six downscaled CCAM simulations all indicate an increasing number of fire days, with the largest increases occurring in the alpine region of Victoria. For the five downscaled GCMs projecting an increase in fire days, the increase in the alpine regions is typically between 20 to 60 days, except for the CCAM-downscaled HadGEM2-CC that projected an increase of 60 to 90 days. The CCAM-downscaled simulations project a smaller increase in the number of fire days for the non-alpine regions in Victoria, with typical increases between 10 to 25 fire days per year. The CCAM-downscaled HadGEM2-CC experiment projected the most extreme increases of 20 to 40 fire days for central and eastern Victoria, with 40 to 50 additional fire days on the eastern coast of Victoria.

A more detailed analysis based on GCMs, NARCLiM and CCAM is still being developed (see NESP Climate Change and Bushfires in Australia, in preparation). However, the majority of CCAM 5km resolution simulations shown here are consistent with the projected average change of the GCM ensemble of typically an increase of 10 to 20 fire days per year for Victoria. However, the downscaled CCAM projections

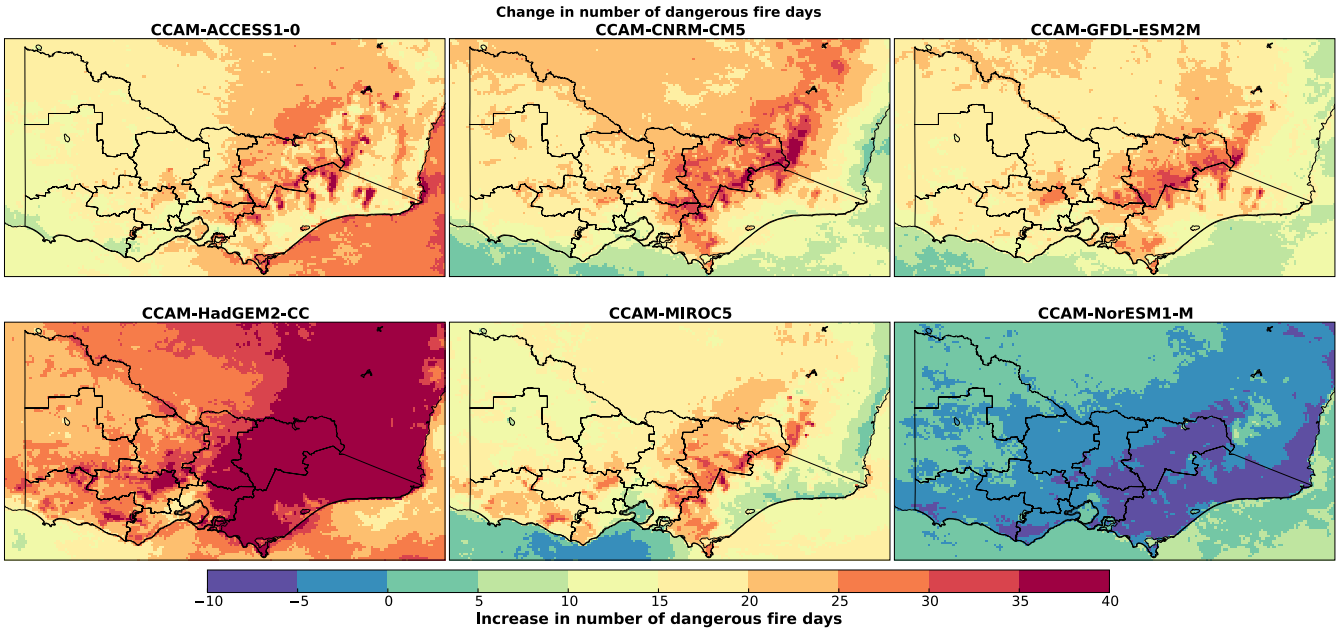

Figure 50. Change in number of fire days per year between 1986–2005 and 2080–2099 under RCP8.5 for the different CCAM downscaled GCMs. Fire days are defined in this report as exceeding the 95th percentile Forest Fire Danger Index (FFDI) for 1986–2005.

have emphasised an increased number of fire days in the alpine regions that can be roughly double the increase in fire days for the non-alpine regions. Further analysis that also includes the other factors that influence fire danger and an analysis more consistent with the Victorian fire ratings will be important for a more complete assessment of changing fire risk.

5.9 Sea level

At large spatial scales, sea levels are influenced by changes in ocean density through heating or cooling of the ocean, and by changes in ocean mass through exchanges with the cryosphere (glaciers and ice sheets) and the terrestrial environment such as soil moisture, lakes and groundwater (CSIRO and Bureau of Meteorology 2015). These large-scale influences can be further modified at the regional scale by effects that act over various time-scales. These include long-term processes such as vertical motion of the land in response to the melting of ice sheets (known as glacial isostatic adjustment, GIA) through to shorter time-scales such as year-to-year (interannual) changes in ocean dynamics driven by climate drivers such as ENSO, and seasonal cycles of changes in 10 m winds and the transfer of heat and fresh water between the ocean and the atmosphere (Church et al. 2011a; CSIRO and Bureau of Meteorology 2015).

As ice sheets and glaciers melt, they alter Earth's gravity field which results in sea-level changes that vary geographically (Mitrovica et al. 2011), meaning that relative sea level is not increasing everywhere on the Earth. It is falling in regions of former ice sheets, rising at faster than the global average rates in adjacent regions, and rising slightly less than the global average in many distant regions (CSIRO and Bureau of Meteorology 2015 and references therein).

Measurements of sea level are obtained via tide gauges and, since 1993, by satellite altimeters. Tide gauge data have indicated that globally sea-level rise has occurred at a rate of 1.7 ± 0.2 mm/yr between 1900 and 2010, with higher rates of rise evident since 1993 confirmed by satellite altimeter data (Church and White 2006; Jevrejeva et al. 2006; Jevrejeva et al. 2008; Church et al. 2011b; Ray and Douglas 2011). From 1993 to 2009, global mean sea-level rise (GMSL) occurred at a rate of 2.8 mm/yr from tide gauge data and 3.4 mm/yr from satellite altimeter data.

Sea-level measurements began in Australia in about 1840 at Port Arthur in Tasmania (Hunter et al. 2003), but the two longest sea-level records are at Fort Denison (Sydney) from 1912 and Fremantle (Western Australia) from 1897.

In Victoria, a citizen science project run by CSIRO in recent years has digitised and quality-controlled paper tide gauge records from Williamstown, extending the useable record back to 1872.

Observed rates of sea-level rise for Australia are consistent with global-average values. After accounting for and removing the effects of vertical land movements due to glacial rebound and the effects of natural climate variability and changes in atmospheric pressure, sea levels have risen around the Australian coastline at an average rate of 2.1 mm/yr from 1966–2009 and 3.1 mm/yr from 1993–2009. There is geographic variation in sea-level rise around Australia, but the trend for the Victorian region is similar to the Australian average (Figure 51). Tide gauge and satellite altimeter trends are generally similar for much of Australia, including the Victorian region. The lower trend at the coast compared with offshore for southeastern Australia is thought to be associated with a strengthening of South Pacific Ocean circulation and southward extension of the East Australian Current.

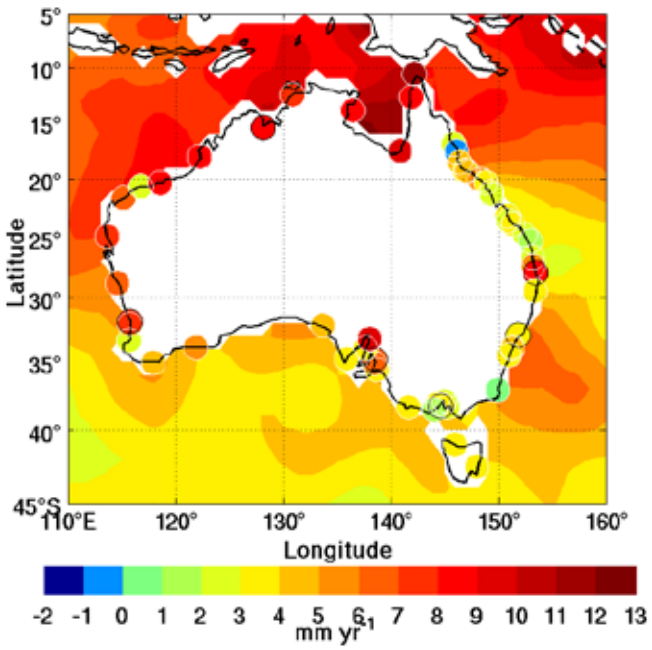

Figure 51. Sea level trends from satellite altimeters (coloured contours) and tide gauges (coloured dots) for 1993 to 2010 after correction for glacial isostatic adjustment. (Source: CSIRO and Bureau of Meteorology 2015)

In the future, the main contributors to sea-level rise are expected to continue to be ocean thermal expansion and loss of glaciers and ice caps, together with loss of ice sheets and changes in the mass of water stored on land. Projections for global mean sea-level rise by the end of the 21st century for RCP2.6 is 0.26–0.55 m (relative to the 1986–2005

baseline), and 0.45–0.82 m under RCP8.5. Projections of sea-level rise for Australia have been made using the methods of Church et al. (2014) and are comparable to the global mean sea-level projections. Projected changes in sea level related to changes in ocean density and circulation (available directly from CMIP5 GCMs) were combined with contributions derived from purpose-built models designed to estimate additional sea level contributions, i.e. from the loss of mass from glaciers, the surface mass balance and the dynamic response of the Greenland and Antarctic ice sheets, changes in land water storage, the mass redistribution from glacier and ice sheet loss and its gravitational response on the ocean, and GIA (CSIRO and Bureau of Meteorology 2015).

National sea-level projections were released in 2015 (CSIRO and Bureau of Meteorology 2015). Tables and maps of projected change under different emissions scenarios and future time periods are available via the *Climate Change in Australia* website[5]. The sea-level data are also available via the *CoastAdapt* website[6] where it has been provided for each coastal council around Australia for four emissions scenarios (RCP2.6, RCP4.5, RCP6.0 and RCP8.5) at five time periods (2030, 2050, 2070, 2090, 2100), as well as a rate of sea-level rise for 2100. Projections for key areas in Victoria were also produced and are available as part of DELWP's *Climate-ready Victoria* brochures[7]. These have been summarised in Table 8 and show projected increases in sea level of around 0.12 m (relative to the baseline period of 1986–2005) by 2030 under medium (RCP4.5) and high (RCP8.5) emissions scenarios. By 2070, the emissions scenario has greater impact, with increases of around 0.32 m under RCP4.5, but up to 0.42 m under RCP8.5. It should be noted that these levels may be higher, depending on the trajectory of Antarctic ice sheet melting in the future (Church et al. 2013). New observations and studies of the role of ice sheet dynamics in future sea-level rise will be quantified in upcoming IPCC assessment reports such as the IPCC Special Report on Oceans and Cryosphere in a Changing Climate (due for release in September 2019).

Sea-level rise not only results in changes in mean sea level, but also contributes to extreme events which are caused by a combination of mean sea level, tides, storm surge, surface waves and coastal geometry. The physical impacts of extreme sea levels on the coast include inundation and erosion. How this might impact Port Phillip Bay in the future is the focus of a DELWP-funded project investigating the likely future hazards of coastal erosion, inundation, and groundwater intrusion. Results will be released in early 2020.

5 www.climatechangeinaustralia.gov.au

6 https://coastadapt.com.au/

7 https://www.climatechange.vic.gov.au/information-and-resources

Table 8. Sea-level rise projections (m) relative to the baseline (1986–2005) for key Victorian locations under medium (RCP4.5) and high (RCP8.5) emissions scenarios for 2030 and 2070. Shown are the median values, with the 5th–95th percentile range given in brackets. (Compiled from Climate-ready Victoria regional data sheets)

Location	2030 RCP4.5	2030 RCP8.5	2070 RCP4.5	2070 RCP8.5
Geelong	0.12 (0.07–0.16)	0.12 (0.08–0.17)	0.32 (0.20–0.45)	0.40 (0.26–0.54)
Point Lonsdale	0.11 (0.07–0.16)	0.12 (0.08–0.17)	0.32 (0.20–0.45)	0.39 (0.25–0.54)
Cape Otway	0.12 (0.07–0.16)	0.12 (0.08–0.17)	0.32 (0.20–0.45)	0.40 (0.26–0.54)
Port Fairy	0.12 (0.08–0.16)	0.13 (0.08–0.17)	0.33 (0.21–0.46)	0.40 (0.26–0.55)
Portland	0.12 (0.08–0.16)	0.13 (0.08–0.18)	0.34 (0.21–0.46)	0.41 (0.27–0.56)
Inverloch	0.12 (0.07–0.16)	0.12 (0.08–0.17)	0.33 (0.21–0.45)	0.40 (0.27–0.54)
Seaspray	0.12 (0.07–0.16)	0.13 (0.08–0.17)	0.33 (0.21–0.45)	0.40 (0.27–0.55)
Marlo	0.12 (0.08–0.17)	0.13 (0.09–0.18)	0.34 (0.22–0.46)	0.42 (0.29–0.56)
Williamstown	0.11 (0.07–0.16)	0.12 (0.08–0.17)	0.32 (0.20–0.45)	0.39 (0.25–0.54)
Stony Point	0.11 (0.07–0.16)	0.12 (0.08–0.17)	0.32 (0.20–0.45)	0.39 (0.25–0.54)

5.10 Step changes

Most climate projections presented in this report give a view of an ongoing climate change signal with climate variability overlaid on it. The climate change signal is presented as a smooth or incremental process, and climate variability is seen as a window or band where the climate varies around this baseline signal. This assumes relative independence of internally-generated climate variability and externally-forced climate change, with a linear combination of the two. However, climate variation and change can appear as steps and jumps rather than a smooth series. The appearance of steps can occur either by an underlying variability and a steadily changing climate combining together to give the appearance of rapid shifts (Figure 52), or true non-linear steps in the climate system (Figure 53). True step changes may be from a rapid transition from one circulation regime to another, also known as a flip between different steady states, such as has been proposed for the southern hemisphere in the late 1970s (Frederiksen and Frederiksen 2011), or from reaching tipping points such as the collapse of ocean circulations, ice sheets or loss of forests (Collins et al. 2013). Here we show an example of temperature, but the same principles also apply to other variables (see also section 5.2.2).

Regardless of the nature of the interaction, the net result is that time-series of climate data can have step change or break points in them. For example, an automated analysis of abrupt change points (detection of where the data do not behave like a linear series) in the mean of Victoria's average annual temperature observations reveals two break points at 1971 and 1999 (Figure 54). Examining climate models, we see that they also simulate these abrupt changes and break points (Figure 55). The simulated break points do not coincide with observed breakpoints unless it is largely driven by an external forcing such as a major volcanic eruption.

For any change, such as a temperature increase or shift in mean rainfall, the change may appear as a relatively stable regime followed by a step-like change, followed by a relatively stable period, and so on. This is particularly important for considering the near-term climate to 2030: if and when there are step-like changes, these may be much more notable and relevant than the smoother change associated with an underlying signal.

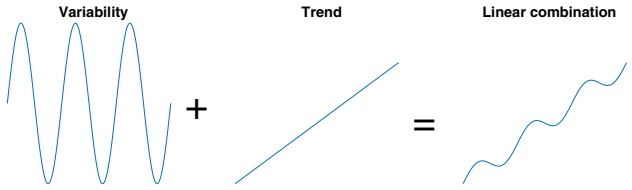

Figure 52. Ongoing variability and a steadily changing climate combining together linearly, creating the appearance of steps.

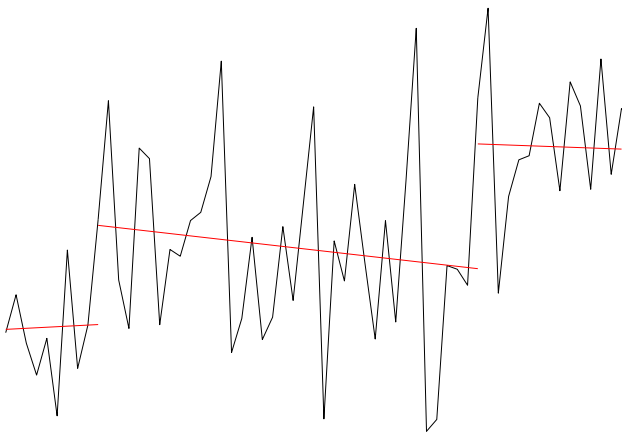

Figure 53. 'Step changes' in the climate system that cannot be seen as a combination of variability and a smooth signal (see Jones and Ricketts (2017) for more discussion of this point).

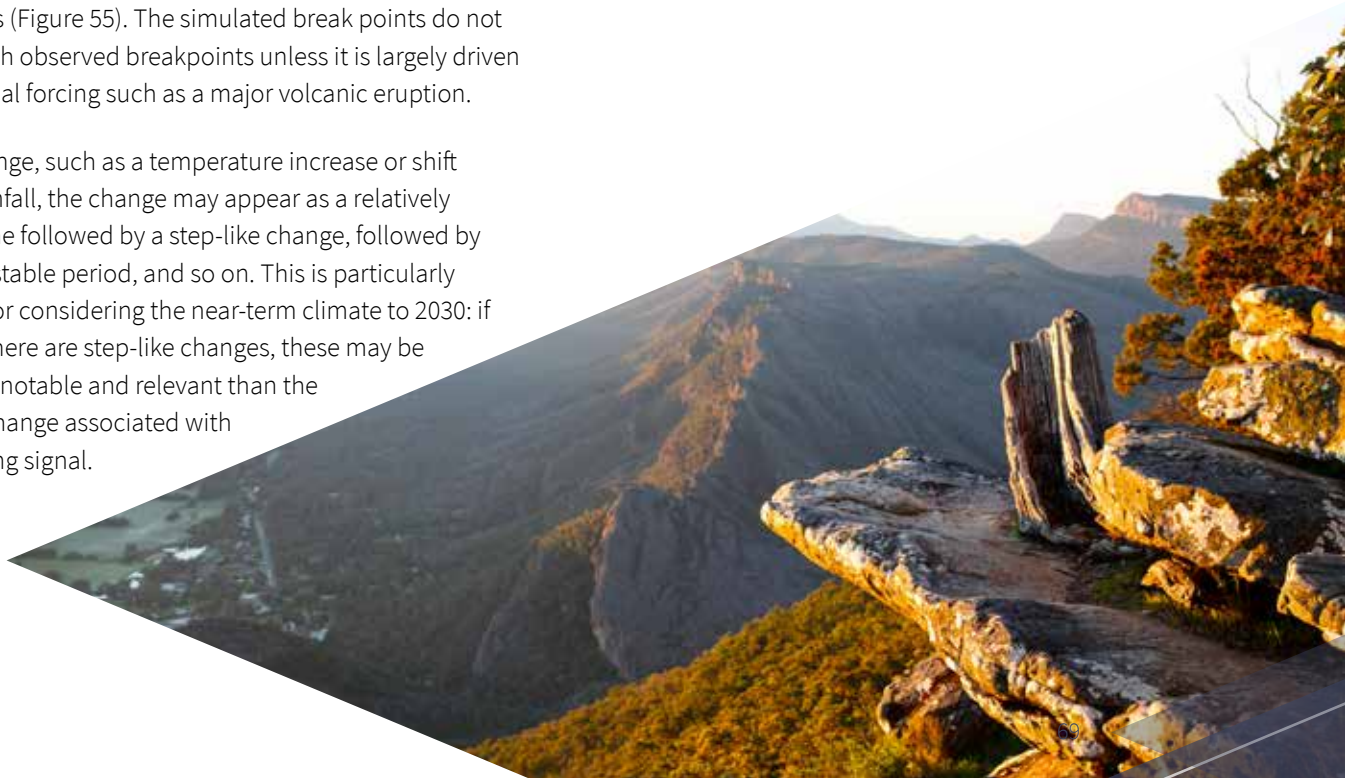

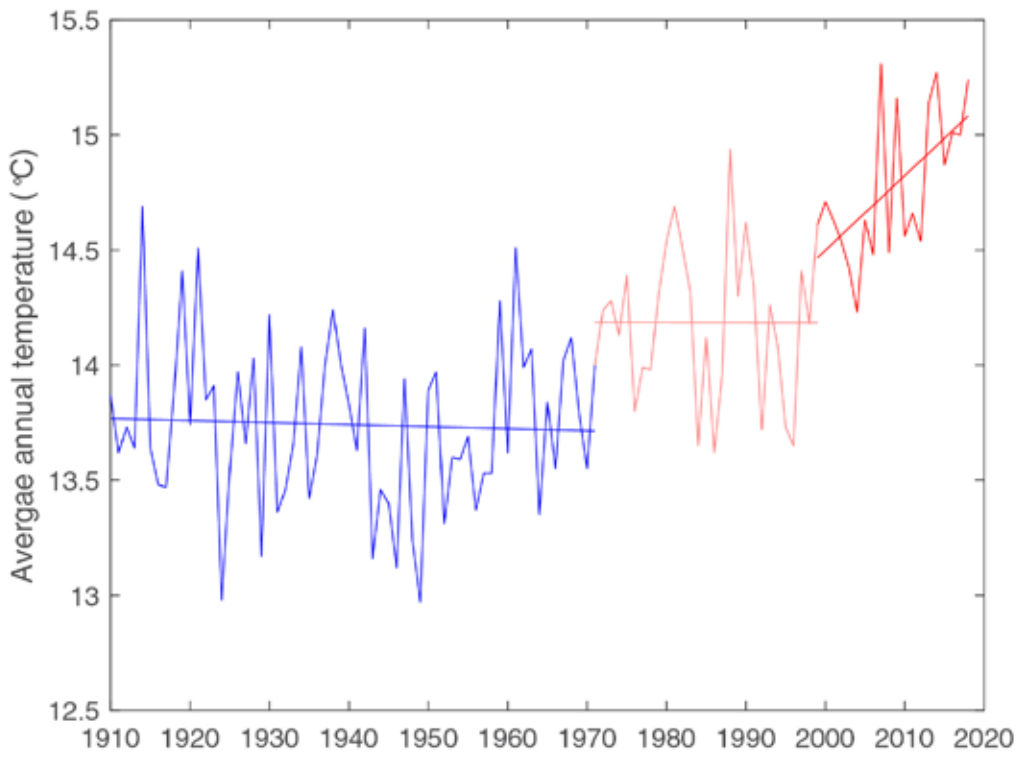

Figure 54. Average annual temperature for Victoria (ACORN-SATv2) showing three eras separated by abrupt change points detected using a breakpoint analysis, and the linear trend in those eras.

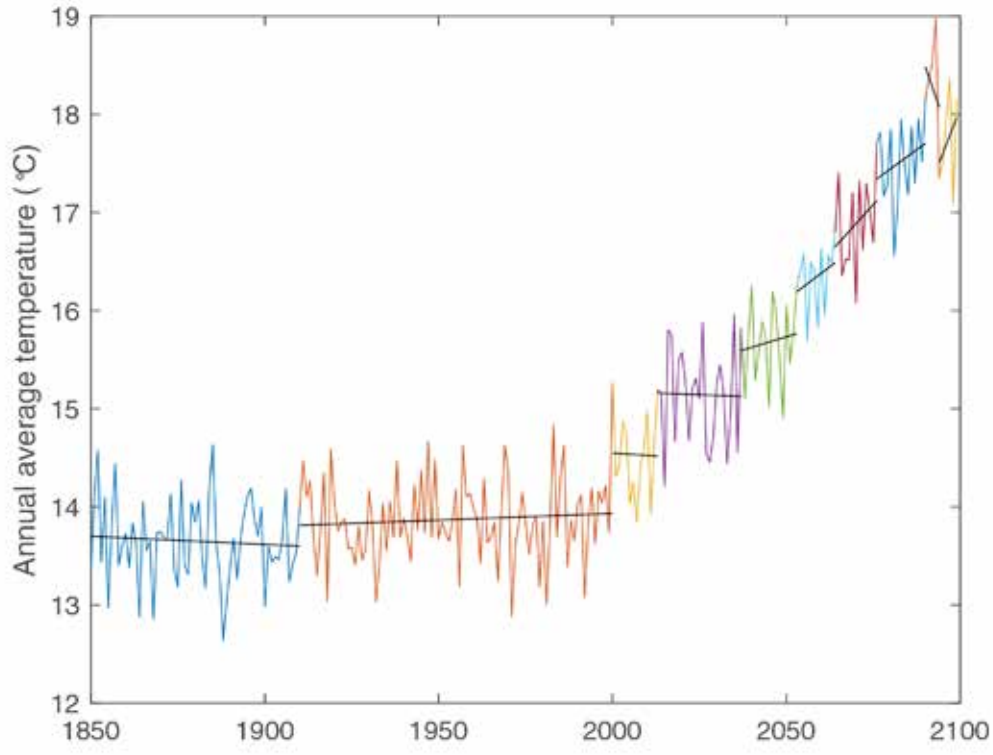

Figure 55. Average annual temperature for Victoria (ACCESS-1.3, RCP8.5) showing 10 eras separated by abrupt change points detected using a breakpoint analysis, and the linear trend in those eras.